

A Regime-Switching Model of the Yield Curve at the Zero Bound

Jens H. E. Christensen[†]

Abstract

This paper presents a regime-switching model of the yield curve with two states: a normal state and a zero-bound state for the case when the monetary policy target rate is at its zero lower bound for a prolonged period, as the U.S. economy has been since December 2008. The model delivers estimates of the time-varying probability of exiting the zero-bound state and can be applied to generate outcome-contingent forecasts useful for portfolio stress tests. The results show that the probability of remaining in the zero-bound state is sensitive to Fed communications, with notable upticks following Federal Reserve decisions to provide further monetary stimulus, whether through asset purchases or forward guidance.

JEL Classification: G12, E43, E52, E58

Keywords: arbitrage-free Nelson-Siegel model, monetary policy, zero lower bound, liftoff probability

I thank Don Kim for helpful comments. Also, I am indebted to Frank Diebold for many helpful comments and suggestions. The views in this paper are solely the responsibility of the author and should not be interpreted as reflecting the views of the Federal Reserve Bank of San Francisco or the Board of Governors of the Federal Reserve System. Finally, I thank James Gillan and Lauren Ford for excellent research assistance.

[†]Contact information: Federal Reserve Bank of San Francisco, 101 Market Street MS 1130, San Francisco, CA 94105, USA; phone: 1-415-974-3115; e-mail: jens.christensen@sf.frb.org.

This version: June 5, 2014.

1 Introduction

Understanding fixed-income markets is important, particularly when traditional monetary policy is at its effective zero lower bound as it has been for the United States since December 2008. Being near the zero boundary poses challenges, one of which is the asymmetry in yield movements. For bond pricing and monetary policy analysis it is critical to account for this asymmetry to accurately capture the yield dynamics near the zero boundary.

The basic premise of the analysis in this paper is that, once the monetary policy target rate hits its nominal zero bound, the dynamics of fixed-income markets change because there are limits to the downside yield movements and, more importantly, the next policy change by the central bank can only be upwards.¹ This leads me to consider a regime-switching model with a normal state and a special state that is referred to as the *zero-bound state*.

A number of papers have tried to model the asymmetry near the zero boundary and its impact on yield curve dynamics. However, most of those papers are either mainly concerned that the model dynamics not violate the zero boundary, or they adjust existing models to work specifically in the zero-bound state (Krippner 2013b and Kim and Singleton 2012 are examples of the former and latter, respectively). They typically do not model a normal and a zero-bound state jointly and the switch between the two.

To understand the features that a model should capture in the zero-bound state and to motivate the model, I first analyze the shift in the statistical properties of the U.S. Treasury yield curve since December 2008, with a particular emphasis on the variation in short-term yields. The analysis reveals that the whole yield curve switches dynamics in the zero-bound state, but the changes are particularly pronounced for yields with less than one year to maturity. As a consequence, U.S. Treasury data seem to call for a fourth factor with a unique role in the short end of the yield curve while in the zero-bound state. Based on this observation, the Treasury yield curve in the normal state is modeled with a standard three-factor term structure model, while the dynamics in the zero-bound state is augmented with a fourth factor that is a square-root process with a special role as detailed in the following.

The key characteristic of the zero-bound state in the model is that the zero bound is given a literal interpretation, that is, while in this regime the instantaneous short rate is constant at zero. To generate variation even in short-term yields, however, there is a positive chance of exiting the zero bound at any time and this is modeled by a time-varying intensity process for a Poisson point process, the first jump of which indicates the exit from the zero bound. In structure, this is similar to the modeling of default events in the reduced-form credit risk

¹The central bank can take other actions at the zero bound such as purchasing long-term assets or provide forward guidance on how long it expects the policy target rate to remain at the zero bound, but these are all just signaling tools that do not change the fundamental fact that when the target rate is at its effective lower bound, the next rate change is up.

literature (Duffie and Singleton 1999 is an excellent example). Theoretically, the zero-bound state is considered an undesirable temporary steady state, and U.S. monetary policymakers are thought to agree, so investors should expect an exit from the zero-bound state, if at all possible. Still, how can the switch out of the zero-bound state be unpredictable at the same time as explicit or extended period forward guidance has been provided by monetary policymakers as has been the case in the United States throughout most of the time spent at the zero bound? In short, there are conditions and states of the world in which even explicit commitments regarding the zero interest rate policy would not be honored. This validates the approach to modeling the exit out of the zero-bound state. From a modeling perspective this is no different than asking how a AAA-rated firm (or a AAA-rated sovereign for that matter) can file for bankruptcy at any given time. The key point is that even though such events appear highly unlikely, they are not impossible. In the context of U.S. monetary policy, one possibility would be for the Federal Open Market Committee (FOMC) not to follow through as stated, which is not likely, but is theoretically possible and consistent with the interpretation given by the FOMC that its policy is state-contingent. Another possibility is that, as new governors are appointed and FOMC voting members rotate, the majority view on the policy committee could change.²

As for the normal state, the probability of switching to the zero-bound state is assumed to be so small, on the order of 0.001 or smaller, that bond investors neglect it for pricing purposes; as such this risk is not reflected in the yield curve in the normal state. The practical implication of this assumption is that bond investors cannot (and did not) foresee a switch to the zero-bound state. Furthermore, and maybe more controversial, a return to the old normal state is assumed whenever the economy leaves the zero-bound state. The motivation for this choice is simple: it is a best guess of what the yield curve dynamics will be after the economy exits the zero-bound state.³ This choice can also be grounded with theoretical considerations. First, there is little evidence to suggest that the way investors process and price information into the Treasury yield curve has changed during the financial crisis.⁴ Second, there has been no change in the way the FOMC operates and communicates its monetary policy decisions. If anything, it has become more transparent, exemplified by the

²The projections of future target rates first published following the January 2012 FOMC meeting do show dispersion in the anticipated appropriate stance of monetary policy among FOMC members over the committed period.

³Krippner (2013a) shows that the arbitrage-free Nelson-Siegel (AFNS) model used for the yield curve in the normal state can be viewed as a close approximation to any Gaussian three-factor model provided the eigenvalues corresponding to the second and third principal components are close. Given that this historically has been the case, there is little to suggest that this would not continue to hold after the exit from the zero-bound state. If so, the AFNS model structure will still deliver a very close approximation to the data, even if the yield curve dynamics obeyed an arbitrary three-factor Gaussian model.

⁴Swanson and Williams (2014) provide evidence that during 2009 and 2010, medium- and long-term Treasury yields have responded to news in much the same way as in the prior decades. This supports the model choice to keep the three factors from the normal state in the zero-bound state.

release of the explicit definition of price stability following the January 2012 FOMC meeting as an annual change of 2 percent in the price index for personal consumption expenditures. And third, the inflation process does not seem to have changed fundamentally despite its low levels in recent years. As such, the response function of the FOMC can be assumed to be constant.⁵ It should be emphasized that the assumption of a return to the old normal state after the exit from the zero-bound state embodies a firm expectation that the FOMC will not raise rates prematurely, that is, without the economy being sufficiently strong to withstand the associated tightening of financial conditions, and hence avoid the double dip scenarios Japan has experienced during its time with near zero yields. Implicitly, once the FOMC exits the zero-bound state, it is expected to stay the course until policy rates have reached more normal levels consistent with conventional monetary policy rules.

Finally, it is assumed that the transition between the two states is observed. In the empirical implementation of the model, this implies that the regime switch to the zero-bound state occurs on December 16, 2008, when the FOMC decided to lock its target rate in the range from 0 to 25 basis points, which represents its effective lower bound, and this was observed by all agents in the economy.

In the empirical analysis, the model is estimated on the full sample. To assess its performance, I compare it to two established three-factor Gaussian models and a more recent three-factor shadow-rate model, where the latter represents an alternative approach to modeling the asymmetric behavior of yields near the zero boundary. First, and most importantly (but not surprisingly), the regime-switching model is observed to outperform the standard and shadow-rate models that impose no regime switch in terms of model fit. In particular, the fit of the short-term yields is improved significantly as expected. Second, it provides a closer match to the compression of short-term yield volatilities in the zero-bound state than the shadow-rate model. Third, the short-rate projections from the regime-switching model are closer to the variation in the rates of federal funds futures than any of the considered alternative models. Fourth, its estimated term premiums are highly correlated with those from the three other models. Thus, overall, the regime-switching model has shown a strong performance during the period the economy has been in the zero-bound state.

Turning to the estimated probability of remaining in the zero-bound state, it is found to be sensitive to Fed communications. For the period until spring 2013, there are notable upward movements in the weeks after major decisions by the FOMC regarding either its large-scale asset purchase (LSAP) programs or its forward guidance for future policy. I interpret this as evidence of a signaling channel in the response of Treasury yields, as also emphasized by Bauer

⁵The very stable ten-year inflation forecasts from the Survey of Professional Forecasters is consistent with this view as it reflects the public's continued trust that the FOMC would counter any significant deviations in the outlook for inflation over the medium-term to ensure that the stated long-run price stability goal would be achieved.

and Rudebusch (2013) and Christensen and Rudebusch (2012, henceforth CR). Consistent with this interpretation, the probability of remaining in the zero-bound state declined over the summer of 2013 when the Fed indicated it was ready to begin to phase out its third and last asset purchase program. Clearly, investors took it as a sign that the end of the zero interest rate policy might be nearer than previously anticipated.

Lastly, the model delivers outcome-contingent forecasts of the future shape of the Treasury yield curve both under the assumption that the economy remains in the zero-bound state and under the assumption that the economy exits the zero-bound state before the end of the forecast horizon. I demonstrate this by making a one-year forecast of the Treasury yield curve as of the end of the sample. This is a useful tool for bond investors in creating realistic scenarios for either outcome. Another potential application could be for stress tests of a bank's portfolio.

There are two research literatures particularly relevant for the analysis in this paper. The first is the nascent, but growing literature on assessing the Fed's exit (or "liftoff" in Fed lingo) from the zero-bound state. A number of papers in this literature combine Gaussian shadow-rate models that respect the zero lower bound for nominal yields with macroeconomic variables (Bauer and Rudebusch 2014 and Wu and Xia 2014 are examples).⁶ Unlike those studies, I rely solely on Treasury yields for model estimation, which allows for high frequency updates and avoids the challenging complication of determining any structural breaks between bond market functioning and real economic variables as a consequence of the zero lower bound on yields.

The second relevant literature, of course, is the vast literature on modeling the yield curve with regime switches. However, unlike that literature where, for tractable pricing, transition probabilities under the risk-neutral Q -measure are at most regime dependent (e.g., Dai et al. 2007 and Koeda 2013), the probability of exiting the zero-bound state in the model introduced in this paper is truly stochastic under both the objective and the risk-neutral probability measures. Technically, the study closest to this paper is the analysis by Piazzesi (2005), who introduced a model in which jumps in the Fed's policy rate are discrete with stochastic intensity but these jumps do not represent a switch in the dynamic structure as in the model described here.

The remainder of the paper is structured as follows. Section 2 describes how U.S. Treasury yields, short-term yields in particular, have behaved at the zero bound relative to the prior normal period. This motivates the regime-switching model introduced in Section 3. Section 4 presents the estimation results, while Section 5 contains a more comprehensive model performance evaluation and Section 6 describes the properties of the asymmetric exit time

⁶Koeda (2013) implements a Gaussian macro-finance model of Japanese bond yields with regime-switches to analyze the time-varying probability of the Bank of Japan leaving its zero interest rate policy.

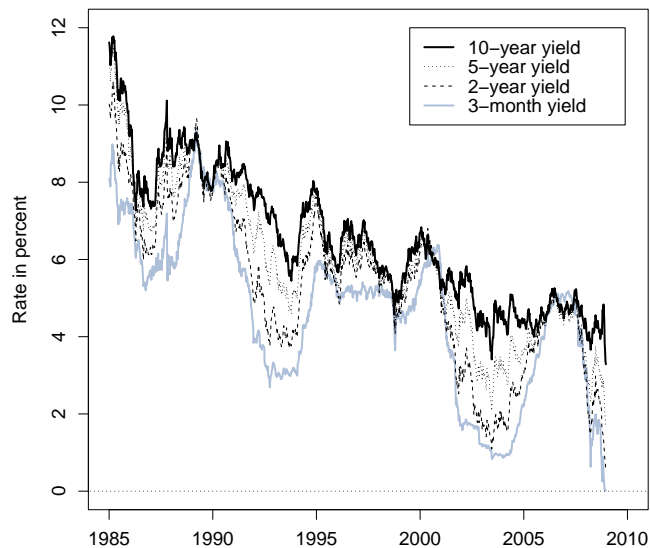


Figure 1: **U.S. Treasury Bond Yields Before December 2008.** Shown are time-series plots of U.S. zero-coupon Treasury bond yields at maturities of 3 months, 2 years, 5 years, and 10 years. The data are weekly from January 4, 1985, to December 12, 2008.

distribution and the yield curve forecasts. Section 7 concludes. Appendices contain technical details on model estimation and the calculation of policy expectations and term premiums.

2 U.S. Treasury Yields in Normal and Zero-Bound States

The yield data used are three- and six-month yields from the H.15 data series combined with one-, two-, three-, five-, seven-, and ten-year yields from the Gürkaynak et al. (2007) database.⁷ The data are continuously compounded zero-coupon yields, measured weekly (Fridays), from January 4, 1985, to December 27, 2013.

2.1 The Treasury Yield Curve in the Normal State

I start with an analysis of the subset of the sample before the FOMC first fixed the target for the overnight federal funds rate in the 0-25 basis point range, that is, before December 16, 2008, which I define as the normal state. Figure 1 shows the variation in four of the eight yield series during this period, while Table 1 reports the summary statistics for this subsample.

⁷Both datasets are available online from the Board of Governors of the Federal Reserve System. See <http://www.federalreserve.gov/releases/h15/> and <http://www.federalreserve.gov/pubs/feds/2006/index.html>.

Maturity (months)	Mean (percent)	Std. dev. (percent)	Skewness	Kurtosis
3	4.68	2.07	-0.15	2.39
6	4.87	2.10	-0.14	2.38
12	5.08	2.11	-0.14	2.35
24	5.37	2.07	-0.04	2.41
36	5.60	2.02	0.08	2.46
60	5.95	1.93	0.28	2.52
84	6.22	1.86	0.41	2.54
120	6.52	1.77	0.51	2.58

Table 1: **Summary Statistics for U.S. Treasury Bond Yields Before December 2008.**

The data are weekly U.S. zero-coupon Treasury bond yields from January 4, 1985, to December 12, 2008, at 8 maturities ranging from 3 months to 10 years. There are $8 \times 1,250$ observations total.

Maturity in months	Loading on			
	First P.C.	Second P.C.	Third P.C.	Fourth P.C.
3	-0.36	-0.44	0.57	-0.47
6	-0.37	-0.40	0.19	0.32
12	-0.38	-0.28	-0.27	0.53
24	-0.38	-0.06	-0.47	-0.05
36	-0.37	0.10	-0.39	-0.36
60	-0.34	0.31	-0.08	-0.33
84	-0.32	0.43	0.17	-0.01
120	-0.30	0.53	0.40	0.40
% explained	94.68	5.04	0.23	0.04

Table 2: **Factor Loadings, U.S. Treasury Bond Yields Before December 2008.**

In the top rows the eigenvectors corresponding to the first four principal components are shown. Put differently, they show how the bond yields at various maturities load on the first four principal components. In the final row the proportion of all bond yield variability explained by each principal component is shown. The data are weekly U.S. zero-coupon Treasury bond yields from January 4, 1985, to December 12, 2008, at eight maturities ranging from 3 months to 10 years. There are $8 \times 1,250$ observations total.

The first observation is that the term structure is upward sloping on average. Second, short- and medium-term yields are more volatile than long-term yields.

Researchers have typically found that three factors are sufficient to model the time-variation in the cross section of U.S. Treasury bond yields (e.g., Litterman and Scheinkman, 1991). Indeed, for the weekly U.S. Treasury bond yield data before mid-December 2008, 99.95% of the total variation is accounted for by three factors. Table 2 reports the eigenvectors that correspond to the first four principal components of the subsample. The first principal component accounts for 94.7% of the variation in the Treasury bond yields, and its loading across maturities is uniformly negative. Thus, like a level factor, a shock to this component changes all yields in the same direction, irrespective of maturity. The second principal component accounts for 5.0% of the variation in these data and has sizable negative loadings for the shorter maturities and sizable positive loadings for the long maturities. Thus,

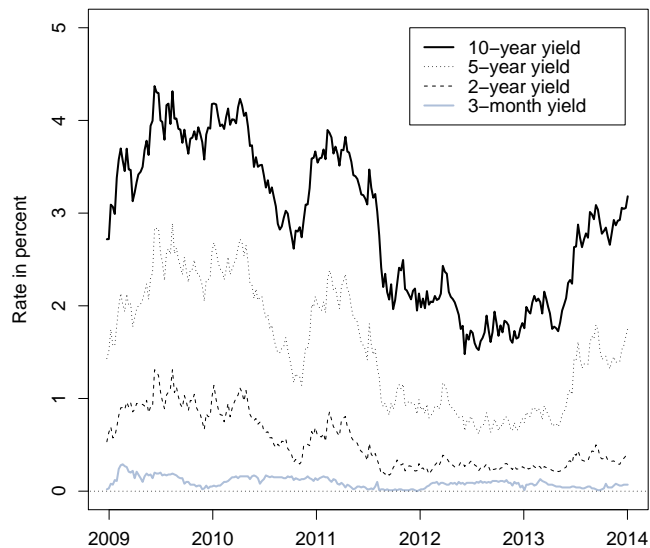


Figure 2: **U.S. Treasury Bond Yields After December 2008.** Shown are time-series plots of U.S. zero-coupon Treasury bond yields at maturities of 3 months, 2 years, 5 years, and 10 years. The data are weekly from December 19, 2008, to December 27, 2013.

like a slope factor, a shock to this component steepens or flattens the yield curve. Finally, the third component, which accounts for 0.2% of the variation, has a U-shaped factor loading as a function of maturity, which is naturally interpreted as a curvature factor. This motivates the use of the Nelson and Siegel (1987) model with its level, slope, and curvature factors for modeling the subsample of U.S. Treasury yields that represent the normal state, even though it should be noted that the estimated state variables are *not* identical to the principal component factors discussed here.⁸ Also, this is consistent with the pre-crisis term structure literature where three factors are widely considered adequate.⁹

2.2 The Treasury Yield Curve in the Zero-Bound State

Now, I repeat the analysis, but focus on the data since the target rate hit the zero bound in mid-December 2008. Figure 2 shows the time variation during this period for the same four yield maturities illustrated in Figure 1. A key distinguishing feature of Treasury yields in the zero-bound state is that medium- and long-term yields can vary significantly at the same time that three- and six-month yields exhibit minimal variation; this is rarely the case

⁸A number of recent papers use principal components as state variables. Joslin et al. (2011) is an example.

⁹Still, there is evidence that three factors may not be sufficient to fully capture all the variation in risk premiums and excess returns, see Cochrane and Piazzesi (2005) and Duffee (2011) for examples and discussions.

Maturity (months)	Mean (percent)	Std. dev. (percent)	Skewness	Kurtosis
3	0.09	0.06	0.64	3.15
6	0.16	0.09	1.15	4.46
12	0.29	0.15	1.05	3.25
24	0.53	0.29	0.69	2.19
36	0.85	0.43	0.48	1.94
60	1.55	0.65	0.20	1.71
84	2.18	0.77	0.05	1.65
120	2.90	0.82	-0.06	1.65

Table 3: **Summary Statistics for U.S. Treasury Bond Yields After December 2008.**

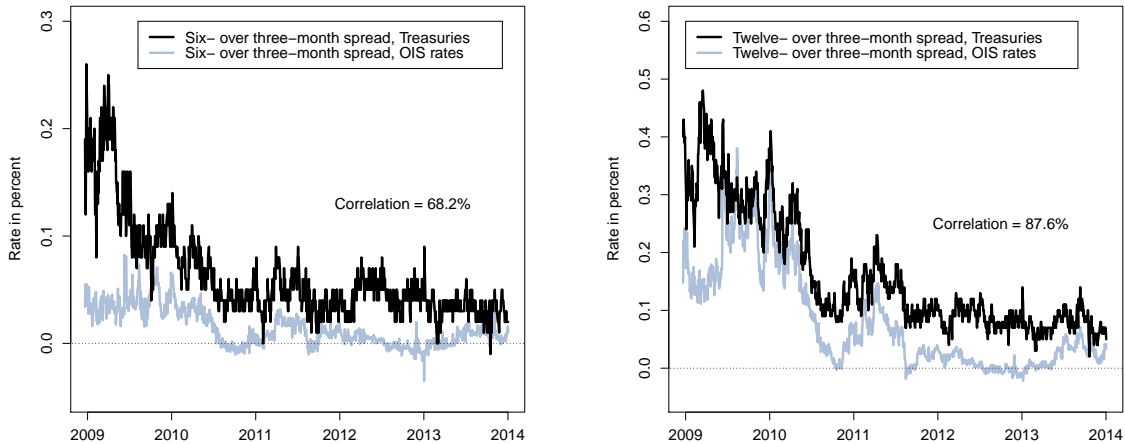
The data are weekly U.S. zero-coupon Treasury bond yields from December 19, 2008, to December 27, 2013, at eight maturities ranging from 3 months to 10 years. There are 8×263 observations total.

Maturity (months)	Loading on			
	First P.C.	Second P.C.	Third P.C.	Fourth P.C.
3	-0.02	-0.16	0.33	0.72
6	-0.04	-0.30	0.48	0.27
12	-0.08	-0.46	0.44	-0.30
24	-0.20	-0.54	-0.08	-0.30
36	-0.31	-0.43	-0.35	-0.03
60	-0.46	-0.09	-0.37	0.31
84	-0.55	0.18	-0.06	0.19
120	-0.59	0.40	0.46	-0.31
% explained	97.71	1.77	0.42	0.07

Table 4: **Factor Loadings, U.S. Treasury Bond Yields After December 2008.** In the top rows the eigenvectors corresponding to the first four principal components are shown. Put differently, they show how the bond yields at various maturities load on the first four principal components. In the final row the proportion of all bond yield variability explained by each principal component is shown. The data are weekly U.S. zero-coupon Treasury bond yields from December 19, 2008, to December 27, 2013, at eight maturities ranging from 3 months to 10 years. There are 8×263 observations total.

in the normal state. Table 3 contains the summary statistics of the yields in the zero-bound state. First, the yield curve continues to be upward sloping, and now systematically so as observed in Figure 2. However, equally important, all yields are less volatile, but obviously the short- to medium-term yields are the ones that have experienced the greatest reduction in yield volatility and are now much less volatile than their long-term counterparts. Thus, a model that accounts for both a normal state and a zero-bound state should replicate this pattern. Furthermore, it should account for the change in the level of interest rates that occur when we move to the zero-bound state.

As in the previous section, I use principal components analysis to better understand the factors driving the variation in the yield curve in the zero-bound state. The result is reported in Table 4. The first three components explain 99.91 percent of the variation, and the loadings on the corresponding eigenvectors across yield maturities have changed though



(a) Spread of six- over three-month yields.

(b) Spread of twelve- over three-month yields.

Figure 3: Short-Term Interest Rate Spreads After December 2008. Panel (a) shows the spreads of six-month over three-month yields for Treasuries and OIS contracts. Panel (b) shows the corresponding spreads of twelve-month over three-month yields. The data are daily from December 16, 2008, to December 31, 2013.

they still reflect a pattern of level, slope, and curvature for medium- to long-term yields. Importantly, it now appears that a fourth factor explains 0.1% of the variation in yields in the zero-bound state and is needed to fully account for the yield dynamics in that state. Furthermore, the loadings on the fourth factor do not have a structure that matches the pattern of either level, slope, or curvature. It has its biggest loading in the very short end of the yield curve (more than twice the size of any of the other loadings). At the same time, the first and second principal components have seen a significant reduction in their loadings on the short-term yields. Thus, it seems that the additional fourth factor is mainly operating in the short end of the curve, where we would expect the biggest changes to the yield curve dynamics to occur when the economy enters the zero-bound state. A good model should account for this pattern in addition to the other stylized facts described above.

2.3 Short Rates in the Zero-Bound State

To get a better sense of the properties of the fourth factor that must be incorporated into the standard three-factor dynamic term structure model, I study the variation in the short end of the U.S. Treasury yield curve in greater detail.

Figure 3(a) shows the variation in the six- over three-month yield spreads from Treasuries and overnight interest swap (OIS) rates, while Figure 3(b) shows the variation in the corresponding twelve- over three-month yield spreads. With correlations in the yield spreads from

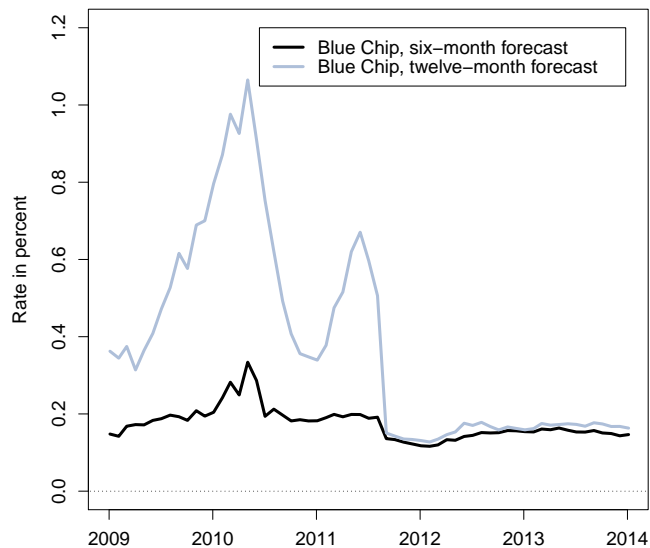


Figure 4: **Blue Chip Federal Funds Rate Survey Forecasts After December 2008.** The Blue Chip survey forecasts refer to the median of the forecasts for the end of each quarter. As a consequence, linear interpolation is used to generate forecasts with constant horizons of 6 and 12 months. The data are monthly from January 1, 2009, to January 1, 2014.

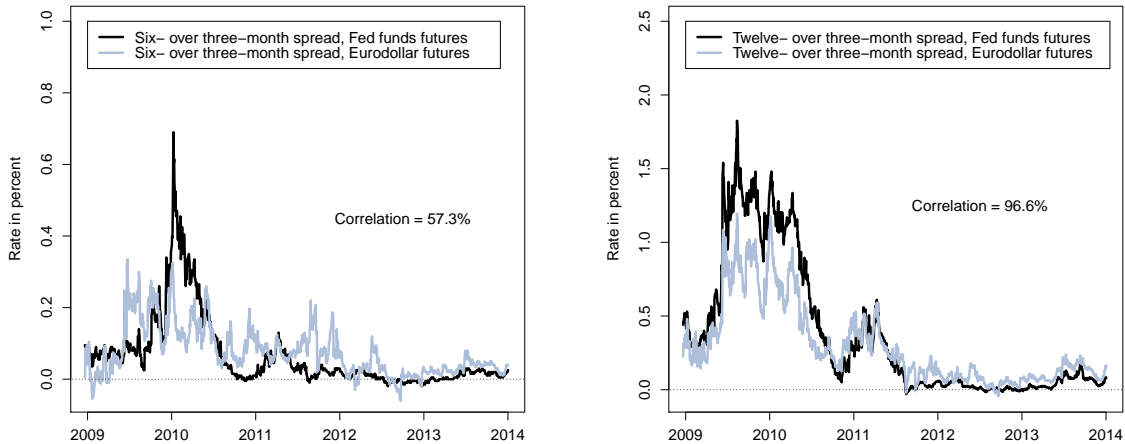
the two curves of 68.2 percent for the six- over three-month spreads and 87.6 percent for the twelve- over three-month yield spreads, it is evident that the specific type of yield data used does not seem to matter for the type of inference we want to make here.¹⁰

Throughout 2011-2013, surveys of primary dealers conducted by the New York Fed indicate that there were effectively no expectations of exiting the zero-bound state within the subsequent six- to twelve-month period.¹¹ Similar low expectations for near-term future monetary policy are reflected in the monthly Blue Chip survey of professional forecasters shown in Figure 4. Thus, the fairly sizable variation in the short-term slope of the yield curve is likely *not* to reflect any material changes in the *expected* future path of monetary policy the following six to twelve months. However, they may well reflect variation in the *uncertainty* about the expected path for future monetary policy over that time horizon and, hence, affect the term premium component of bond yields.

Figure 5(a) reveals notable variation in the six- over three-month spreads of rates on

¹⁰It should be noted that if OIS rates are used in model estimation, a parsimonious term structure model could have some difficulty replicating the occasional negative slope of the short end of the OIS curve, which does not occur in the Treasury data sample. However, these slight inversions are likely the result of microstructure noise rather than investor expectations.

¹¹The questions and responses from the New York Fed's survey of primary dealers are available at: http://www.newyorkfed.org/markets/primarydealer_survey_questions.html.



(a) Spread of six- over three-month futures.

(b) Spread of twelve- over three-month futures.

Figure 5: Spreads of Short-Term Futures Rates After December 2008. Panel (a) shows the spreads of six-month over three-month rates on federal funds and Eurodollar futures contracts. Panel (b) shows the corresponding spreads of twelve-month over three-month futures rates. The data are daily from December 16, 2008, to December 31, 2013.

federal funds and eurodollar futures contracts, while Figure 5(b) reveals even larger variation in the twelve- over three-month spreads of the futures rates. Combined with the observations above, this is evidence that term premiums are likely to be as large and volatile near the zero bound as they are in the normal state.¹² The regime-switching model introduced in the following section accommodates this aspect of the data by letting the added fourth factor be a square-root process that can generate the kind of stochastic short-term yield volatility seen in Figures 3 and 5, even though the instantaneous risk-free rate is constant at zero. Furthermore, it is important to emphasize that the objective is to create a model that accurately describes the Treasury yield curve before it reaches the zero bound, while at the zero bound, and after the exit from the zero bound.

3 Model Description

This section describes the regime-switching model studied in the remainder of the paper.

In the normal state, the yield curve is characterized by its usual level, slope, and curvature factor, here denoted (L_t, S_t, C_t) , which are modeled using the arbitrage-free Nelson-Siegel (AFNS) model introduced in Christensen et al. (CDR, 2011).¹³ To preserve the Nelson-

¹²Piazzesi and Swanson (2008) provide evidence of large and time-varying risk premiums in the rates of federal funds futures contracts in the normal pre-crisis period.

¹³See Diebold and Rudebusch (2013) for a comprehensive presentation of related applications of the AFNS model.

Siegel factor loading structure in the yield function, the instantaneous risk-free rate is defined as:

$$r_t = L_t + S_t.$$

Furthermore, the risk-neutral (or Q -) dynamics of the state variables are given by the following system of stochastic differential equations:¹⁴

$$\begin{pmatrix} dL_t \\ dS_t \\ dC_t \end{pmatrix} = \begin{pmatrix} 0 & 0 & 0 \\ 0 & -\lambda & \lambda \\ 0 & 0 & -\lambda \end{pmatrix} \begin{pmatrix} L_t \\ S_t \\ C_t \end{pmatrix} dt + \Sigma \begin{pmatrix} dW_t^{L,Q} \\ dW_t^{S,Q} \\ dW_t^{C,Q} \end{pmatrix},$$

where Σ is the constant covariance (or volatility) matrix.¹⁵ Based on this specification of the Q -dynamics, zero-coupon bond yields in the normal state preserve the popular Nelson and Siegel (1987) factor loading structure as

$$y_t^N(\tau) = L_t + \left(\frac{1 - e^{-\lambda\tau}}{\lambda\tau} \right) S_t + \left(\frac{1 - e^{-\lambda\tau}}{\lambda\tau} - e^{-\lambda\tau} \right) C_t - \frac{A^N(\tau)}{\tau}, \quad (1)$$

where $A^N(\tau)/\tau$ is a maturity-dependent yield-adjustment term that applies in the normal state.¹⁶

The zero-bound state has two salient features. First, the instantaneous short rate is assumed constant and fixed at zero, to be consistent with the data.¹⁷ Second, it is assumed that there is an additional state variable that drives the variation in the intensity process for the Poisson jump process that indicates the switch out of the zero-bound state. This process is denoted η_t and is assumed to follow a square-root process to preserve strict positivity:

$$d\eta_t = \kappa_\eta^Q (\theta_\eta^Q - \eta_t) dt + \sigma_\eta \sqrt{\eta_t} dW_t^{\eta,Q}.$$

The implication of this modeling approach is that the switch from the zero-bound state back to the normal state is unpredictable, even in the days before the actual announcement. This modeling choice can be defended in two ways. First, from December 2008 until August 2011, the FOMC only used “extended period” language so it was left to anybody’s guess as

¹⁴As discussed in CDR, with a unit root in the level factor under the pricing probability measure, the model is not arbitrage-free with an unbounded horizon; therefore, as is often done in theoretical discussions, an arbitrary maximum horizon is imposed.

¹⁵As per CDR, Σ is a diagonal matrix, and θ^Q is set to zero without loss of generality.

¹⁶CDR provide the analytical formula for $A^N(\tau)/\tau$.

¹⁷In the daily H.15 database through 2013 (of which I use a weekly subsample), the zero boundary is *never* violated. The one-month yield is 0 on 43 dates, the three-month yield is 0 on 8 dates, while the six-month yield never goes below 2 basis points. Furthermore, since late 2008, the spread between the six- and three-month yields is always positive except for four days, on one of which it was negative 1 basis point (October 11, 2013). Thus, with three- and six-month yields less than 10 basis points and the yield curve steep for much of the time spent in the zero-bound state, the choice of zero for the short rate appears to be a reasonable assumption, if not outright the true value.

to what defined an extended period. Thus, during this period, the exact switch date could not be foreseen. Second, after August 2011 when explicit forward guidance was introduced, it was still uncertain whether the zero-bound period would extend beyond the explicit future date or even whether the FOMC would change its mind before reaching that date. Thus, in reality, it was never completely certain when and how the FOMC would exit the zero-bound state and, as shown by Duffie and Lando (2001), with this kind of uncertainty surrounding what might otherwise be a predictable event, it is theoretically consistent to model it as an unpredictable event with a stochastic intensity process that reflects the time-varying chance of exiting the zero-bound state at any given time.

Since the principal components decomposition of the Treasury yield curve since December 19, 2008, shown in Table 4 continues to reflect a structure with level, slope, and curvature, the dynamics of the three regular state variables are assumed not to change when the economy switches to the zero-bound state. As a consequence, the dynamics of the state variables under the pricing Q -measure in the zero-bound state are assumed to be driven by the following system of stochastic differential equations:

$$\begin{aligned} \begin{pmatrix} dL_t \\ dS_t \\ dC_t \\ d\eta_t \end{pmatrix} &= \begin{pmatrix} 0 & 0 & 0 & 0 \\ 0 & \lambda & -\lambda & 0 \\ 0 & 0 & \lambda & 0 \\ 0 & 0 & 0 & \kappa_\eta^Q \end{pmatrix} \left[\begin{pmatrix} 0 \\ 0 \\ 0 \\ \theta_\eta^Q \end{pmatrix} - \begin{pmatrix} L_t \\ S_t \\ C_t \\ \eta_t \end{pmatrix} \right] dt \\ &+ \begin{pmatrix} \sigma_L & 0 & 0 & 0 \\ 0 & \sigma_S & 0 & 0 \\ 0 & 0 & \sigma_C & 0 \\ 0 & 0 & 0 & \sigma_\eta \end{pmatrix} \begin{pmatrix} \sqrt{1} & 0 & 0 & 0 \\ 0 & \sqrt{1} & 0 & 0 \\ 0 & 0 & \sqrt{1} & 0 \\ 0 & 0 & 0 & \sqrt{\eta_t} \end{pmatrix} \begin{pmatrix} dW_t^{L,Q} \\ dW_t^{S,Q} \\ dW_t^{C,Q} \\ dW_t^{\eta,Q} \end{pmatrix}. \end{aligned}$$

In the zero-bound state, zero-coupon bond prices are calculated as follows:

$$\begin{aligned} P^Z(t, T) &= E_t^Q \left[e^{-\int_t^T r_u du} \right] \\ &= E_t^Q \left[\mathbf{1}_{\{\text{In } Z \text{ state at } T\}} + \int_t^T \mathbf{1}_{\{\text{Exit } Z \text{ state at } s\}} e^{-\int_s^T r_u du} ds \right] \\ &= E_t^Q \left[e^{-\int_t^T \eta_u du} \right] + E_t^Q \left[\int_t^T \eta_s e^{-\int_t^s \eta_u du} e^{-\int_s^T r_u du} ds \right] \\ &= E_t^Q \left[e^{-\int_t^T \eta_u du} \right] + \int_t^T E_t^Q \left[\eta_s e^{-\int_t^s \eta_u du} E_s^Q \left[e^{-\int_s^T r_u du} \right] \right] ds \\ &= E_t^Q \left[e^{-\int_t^T \eta_u du} \right] \\ &\quad + \int_t^T E_t^Q \left[\eta_s e^{-\int_t^s \eta_u du} e^{A^N(s,T) + B_L^N(s,T)L_s + B_S^N(s,T)S_s + B_C^N(s,T)C_s} \right] ds. \end{aligned}$$

The first term is the probability of remaining in the zero-bound state beyond time T in which case discounting is done throughout at zero interest. The second term is the cumulative probability of exiting the zero-bound state prior to time T multiplied by risk-neutral discounting using the normal-state dynamics of the short rate over the remaining time until T .

The formulas needed to calculate the above expectations are provided in the following proposition.¹⁸

Proposition 1:

In the zero-bound state, zero-coupon bond prices are calculated as follows:

$$P^Z(t, T) = E_t^Q \left[e^{-\int_t^T \eta_u du} \right] + \int_t^T E_t^Q \left[\eta_s e^{-\int_t^s \eta_u du} e^{A^N(s, T) + B_L^N(s, T)L_s + B_S^N(s, T)S_s + B_C^N(s, T)C_s} \right] ds,$$

where

$$E_t^Q \left[e^{-\int_t^T \eta_u du} \right] = \exp \left(A_\eta(t, T) + B_\eta(t, T)\eta_t \right), \quad (2)$$

$$A_\eta(t, T) = \frac{2\kappa_\eta^Q \theta_\eta^Q}{\sigma_\eta^2} \ln \left[\frac{2\phi_\eta e^{\frac{1}{2}(\phi_\eta + \kappa_\eta^Q)(T-t)}}{2\phi_\eta + (\phi_\eta + \kappa_\eta^Q)(e^{\phi_\eta(T-t)} - 1)} \right], \quad (3)$$

$$B_\eta(t, T) = \frac{-2(e^{\phi_\eta(T-t)} - 1)}{2\phi_\eta + (\phi_\eta + \kappa_\eta^Q)[e^{\phi_\eta(T-t)} - 1]}, \quad (4)$$

and

$$\begin{aligned} & E_t^Q \left[\eta_s e^{-\int_t^s \eta_u du} e^{A^N(s, T) + B_L^N(s, T)L_s + B_S^N(s, T)S_s + B_C^N(s, T)C_s} \right] \\ &= \exp \left(A^Z(t, s, T) + B_L^Z(t, s, T)L_t + B_S^Z(t, s, T)S_t + B_C^Z(t, s, T)C_t + B_\eta^Z(t, s, T)\eta_t \right) \\ & \quad \times \left[C^Z(t, s, T) + D_\eta^Z(t, s, T)\eta_t \right] \end{aligned}$$

¹⁸The calculations leading to the formulas in Proposition 1 are available upon request.

with

$$\begin{aligned}
A^Z(t, s, T) &= \bar{A}^N(s, T) + \frac{\sigma_L^2}{2} \bar{B}_L^N(s, T)^2 (s-t) + \frac{\sigma_S^2}{2} \bar{B}_S^N(s, T)^2 \frac{1 - e^{-\lambda(s-t)}}{\lambda} \\
&\quad + \sigma_C^2 \bar{B}_C^N(s, T)^2 \frac{1 - e^{-2\lambda(s-t)}}{4\lambda} \\
&\quad + \frac{\sigma_C^2}{2} \bar{B}_C^N(s, T)^2 \left[-\frac{1}{2} \lambda (s-t)^2 e^{-2\lambda(s-t)} - \frac{1}{2} (s-t) e^{-2\lambda(s-t)} + \frac{1 - e^{-2\lambda(s-t)}}{4\lambda} \right] \\
&\quad + \sigma_C^2 \lambda \bar{B}_S^N(s, T) \bar{B}_C^N(s, T) \left[-\frac{1}{2\lambda} (s-t) e^{-2\lambda(s-t)} + \frac{1 - e^{-2\lambda(s-t)}}{4\lambda^2} \right] \\
&\quad + \frac{2\kappa_\eta^Q \theta_\eta^Q}{\sigma_\eta^2} \ln \left[\frac{2\phi_\eta e^{\frac{1}{2}(\phi_\eta + \kappa_\eta^Q)(s-t)}}{2\phi_\eta + (\phi_\eta + \kappa_\eta^Q)(e^{\phi_\eta(s-t)} - 1)} \right], \\
B_L^Z(t, s, T) &= \bar{B}_L^N(s, T), \\
B_S^Z(t, s, T) &= e^{-\lambda(s-t)} \bar{B}_S^N(s, T), \\
B_C^Z(t, s, T) &= e^{-\lambda(s-t)} \bar{B}_C^N(s, T) + \lambda(s-t) e^{-\lambda(s-t)} \bar{B}_S^N(s, T), \\
B_\eta^Z(t, s, T) &= \frac{-2(e^{\phi_\eta(s-t)} - 1)}{2\phi_\eta + (\phi_\eta + \kappa_\eta^Q)[e^{\phi_\eta(s-t)} - 1]}, \\
C^Z(t, s, T) &= \frac{2\kappa_\eta^Q \theta_\eta^Q \bar{D}_\eta(s, T)(e^{\phi_\eta(s-t)} - 1)}{2\phi_\eta + (\phi_\eta + \kappa_\eta^Q)(e^{\phi_\eta(s-t)} - 1)}, \\
D_\eta^Z(t, s, T) &= \frac{4\phi_\eta^2 e^{\phi_\eta(s-t)} \bar{D}_\eta(s, T)}{[2\phi_\eta + (\phi_\eta + \kappa_\eta^Q)(e^{\phi_\eta(s-t)} - 1)]^2}.
\end{aligned}$$

Finally, the boundary values in the formulas above are:

$$\begin{aligned}
\bar{A}^N(s, T) &= \sigma_L^2 \frac{(T-s)^3}{6} + \sigma_S^2 \left[\frac{1}{2\lambda^2} (T-s) - \frac{1}{\lambda^3} (1 - e^{-\lambda(T-s)}) + \frac{1}{4\lambda^3} (1 - e^{-2\lambda(T-s)}) \right] \\
&\quad + \sigma_C^2 \left[\frac{1}{2\lambda^2} (T-s) + \frac{1}{\lambda^2} (T-s) e^{-\lambda(T-s)} - \frac{1}{4\lambda} (T-s)^2 e^{-2\lambda(T-s)} \right. \\
&\quad \quad \left. - \frac{3}{4\lambda^2} (T-s) e^{-2\lambda(T-s)} - \frac{2}{\lambda^3} (1 - e^{-\lambda(T-s)}) + \frac{5}{8\lambda^3} (1 - e^{-2\lambda(T-s)}) \right], \\
\bar{B}_L^N(s, T) &= -(T-s), \\
\bar{B}_S^N(s, T) &= -\frac{1 - e^{-\lambda(T-s)}}{\lambda}, \\
\bar{B}_C^N(s, T) &= (T-s) e^{-\lambda(T-s)} - \frac{1 - e^{-\lambda(T-s)}}{\lambda}, \\
\bar{D}_\eta(s, T) &= 1.
\end{aligned}$$

Throughout it holds that

$$\phi_\eta = \sqrt{(\kappa_\eta^Q)^2 + 2\sigma_\eta^2}.$$

It is noted that zero-coupon bond prices in both regimes are known in analytical form

(up to the calculation of a single integral in the maturity dimension), which facilitates the empirical implementation of the model. Also, applying the formulas in Proposition 1, zero-coupon bond yields in the zero-bound state are easily calculated as

$$y^Z(t, T) = -\frac{1}{T-t} \ln P^Z(t, T). \quad (5)$$

To complete the model, the risk premium structure that provides the connection between the pricing dynamics described above and the real-world dynamics of the state variables needs to be specified. Using the extended affine risk premiums introduced in Cheridito et al. (2007), the maximally flexible specification of the model has P -dynamics given by

$$\begin{aligned} \begin{pmatrix} dL_t \\ dS_t \\ dC_t \\ d\eta_t \end{pmatrix} &= \begin{pmatrix} \kappa_{11}^P & \kappa_{12}^P & \kappa_{13}^P & \kappa_{14}^P \\ \kappa_{21}^P & \kappa_{22}^P & \kappa_{23}^P & \kappa_{24}^P \\ \kappa_{31}^P & \kappa_{32}^P & \kappa_{33}^P & \kappa_{34}^P \\ 0 & 0 & 0 & \kappa_{44}^P \end{pmatrix} \left[\begin{pmatrix} \theta_1^P \\ \theta_2^P \\ \theta_3^P \\ \theta_4^P \end{pmatrix} - \begin{pmatrix} L_t \\ S_t \\ C_t \\ \eta_t \end{pmatrix} \right] dt \\ &+ \begin{pmatrix} \sigma_L & 0 & 0 & 0 \\ 0 & \sigma_S & 0 & 0 \\ 0 & 0 & \sigma_C & 0 \\ 0 & 0 & 0 & \sigma_\eta \end{pmatrix} \begin{pmatrix} \sqrt{1} & 0 & 0 & 0 \\ 0 & \sqrt{1} & 0 & 0 \\ 0 & 0 & \sqrt{1} & 0 \\ 0 & 0 & 0 & \sqrt{\eta_t} \end{pmatrix} \begin{pmatrix} dW_t^{L,P} \\ dW_t^{S,P} \\ dW_t^{C,P} \\ dW_t^{\eta,P} \end{pmatrix}. \end{aligned}$$

Similar to the approach for the Q -dynamics used for pricing, the P -dynamics of the level, slope, and curvature are assumed to remain the same throughout. However, a switch in the P -dynamics of the first three factors, when in the zero-bound state, can easily be incorporated if deemed appropriate.¹⁹

Finally, the model estimation is based on the Kalman filter and described in Appendix A.

4 Estimation Results

In this section, I describe the regime-switching model selection and the estimation results, while a more comprehensive performance evaluation is left for the subsequent section.

For estimating the probability of exiting the zero-bound state, as well as for forecasting, the specification of the mean-reversion matrix K^P is critical. To select the best fitting specification of the model's real-world dynamics, I use a general-to-specific modeling strategy that restricts the least significant off-diagonal parameter of K^P to zero and then re-estimates the model. This strategy of eliminating the least significant coefficients is carried out down to the most

¹⁹The practical problem in imposing a regime switch on the upper three-dimensional part of K^P , θ^P , and Σ is twofold. First, it increases the number of parameters significantly. Second, and more importantly, there is only a short sample to identify these additional parameters from, which prevents efficient estimation.

Alternative specifications	Goodness-of-fit statistics				
	$\log L$	k	p -value	AIC	BIC
(1) Unrestricted K^P	70,437.47	40	n.a.	-140,794.9	-140,699.2
(2) $\kappa_{14}^P = 0$	70,437.35	39	0.6242	-140,796.7	-140,589.1
(3) $\kappa_{14}^P = \kappa_{31}^P = 0$	70,437.18	38	0.5598	-140,798.4	-140,596.1
(4) $\kappa_{14}^P = \kappa_{31}^P = \kappa_{32}^P = 0$	70,436.52	37	0.3032	-140,799.0	-140,602.1
(5) $\kappa_{14}^P = \dots = \kappa_{21}^P = 0$	70,434.58	36	0.0489	-140,797.2	-140,605.6
(6) $\kappa_{14}^P = \dots = \kappa_{12}^P = 0$	70,432.72	35	0.0538	-140,795.4	-140,609.2
(7) $\kappa_{14}^P = \dots = \kappa_{34}^P = 0$	70,431.62	34	0.1380	-140,795.2	-140,614.3
(8) $\kappa_{14}^P = \dots = \kappa_{24}^P = 0$	70,426.55	33	0.0015	-140,787.1	-140,611.5
(9) $\kappa_{14}^P = \dots = \kappa_{23}^P = 0$	70,423.76	32	0.0182	-140,783.5	-140,613.2
(10) $\kappa_{14}^P = \dots = \kappa_{13}^P = 0$	70,420.63	31	0.0123	-140,779.3	-140,614.3

Table 5: **Evaluation of Alternative Specifications of the Regime-Switching Model.**

Ten alternative estimated specifications of the regime-switching model are evaluated. Each specification is listed with its maximum log likelihood ($\log L$), number of parameters (k), and the p -value from a likelihood ratio test of the hypothesis that the specification differs from the one directly above that has one more free parameter. The information criteria (AIC and BIC) are also reported, and their minimum values are given in boldface.

parsimonious specification, which has a diagonal K^P matrix. The final specification choice is based on the values of the Akaike and Bayes information criteria as per Christensen et al. (2010) (see, e.g., Harvey 1989).²⁰

The summary statistics of the model selection process are reported in Table 5. The Akaike information criterion is minimized by specification (4), which has a K^P matrix given by

$$K_{AIC}^P = \begin{pmatrix} \kappa_{11}^P & \kappa_{12}^P & \kappa_{13}^P & 0 \\ \kappa_{21}^P & \kappa_{22}^P & \kappa_{23}^P & \kappa_{24}^P \\ 0 & 0 & \kappa_{33}^P & \kappa_{34}^P \\ 0 & 0 & 0 & \kappa_{44}^P \end{pmatrix},$$

while the Bayes information criterion prefers the more parsimonious specification (7) with a K^P matrix given by

$$K_{BIC}^P = \begin{pmatrix} \kappa_{11}^P & 0 & \kappa_{13}^P & 0 \\ 0 & \kappa_{22}^P & \kappa_{23}^P & \kappa_{24}^P \\ 0 & 0 & \kappa_{33}^P & 0 \\ 0 & 0 & 0 & \kappa_{44}^P \end{pmatrix}.$$

In light of the relatively low number of observations from the zero-bound state, the BIC

²⁰The Akaike information criterion is defined as $AIC = -2\log L + 2k$, where k is the number of model parameters, while the Bayes information criterion is defined as $BIC = -2\log L + k \log T$, where T is the number of data observations. The data set contains 1,513 weekly observations for the full sample, but only 263 observations of η_t in the zero-bound state. Still, T is interpreted as referring to the longest data series and is fixed at 1,513.

K^P	$K_{\cdot,1}^P$	$K_{\cdot,2}^P$	$K_{\cdot,3}^P$	$K_{\cdot,4}^P$	θ^P		Σ
$K_{1,\cdot}^P$	0.3275 (0.0975)	0.1141 (0.0835)	-0.1532 (0.0504)	0	0.0702 (0.0051)	σ_L	0.0069 (0.0001)
$K_{2,\cdot}^P$	0.2200 (0.1982)	0.3375 (0.1603)	-0.3852 (0.1201)	0.0266 (0.0091)	-0.0320 (0.0124)	σ_S	0.0110 (0.0002)
$K_{3,\cdot}^P$	0	0	0.9260 (0.2054)	-0.0696 (0.0270)	-0.0187 (0.0056)	σ_C	0.0273 (0.0005)
$K_{4,\cdot}^P$	0	0	0	0.4060 (0.2496)	1.0309 (0.0948)	σ_η	0.9149 (0.0596)

Table 6: **Estimated Parameters in Regime-Switching Model.** The estimated parameters of the K^P matrix, θ^P vector, and diagonal Σ matrix for the regime-switching model are shown. The estimated value of λ is 0.4740 (0.0027), while $\kappa_\eta^Q = 0.0991$ (0.1419) and $\theta_\eta^Q = 6.4520$ (0.7419). The numbers in parentheses are the estimated parameter standard deviations. The maximum log likelihood value is 70,436.52.

might impose a penalty for including additional parameters that is too large. For that reason I choose to focus on the specification preferred by AIC in the remainder of the paper.

For the upper 3×3 part of the mean-reversion matrix K^P , that represents the factor dynamics in the normal state, the preferred specification is nesting the specification favored by CR, who went through a careful and extensive model selection process to find a well-specified AFNS model of U.S. Treasury yields for the 1987-2010 period.²¹ However, they impose a unit-root property on the Nelson-Siegel level factor to improve forecast performance and mitigate issues related to the finite-sample upward bias in the estimated parameters of the K^P mean-reversion matrix.²² I choose not to do that as it seems to interfere with the estimation of the off-diagonal elements in the fourth column of K^P . Furthermore, due to the long sample and the estimated high persistence of the state variables, there would likely only be modest gains from correcting for the finite-sample bias in the estimated parameters of K^P , which would not warrant the added computational burden.

Table 6 contains the estimated model parameters. As noted above, the level factor is the most persistent factor. The slope factor is also very persistent with a rate of mean-reversion of around 0.35, while the curvature factor is less persistent and more volatile. Finally, the η_t intensity process for the switch out of the zero-bound state is slightly less persistent than the slope factor, but more persistent than the curvature factor.

In the remainder of this subsection, additional estimation results from the regime-switching model are studied in some detail and compared to those obtained from estimating the standard AFNS model that preserves the normal-state dynamics in the preferred specification of the regime-switching model throughout.²³

²¹The difference relative to their specification is that they impose two additional restrictions: $\kappa_{12}^P = \kappa_{13}^P = 0$.

²²See Bauer et al. (2012) for a detailed discussion of this problem in the context of Gaussian dynamic term structure models.

²³It is worth emphasizing that none of the results discussed are sensitive to the specific choice of mean-

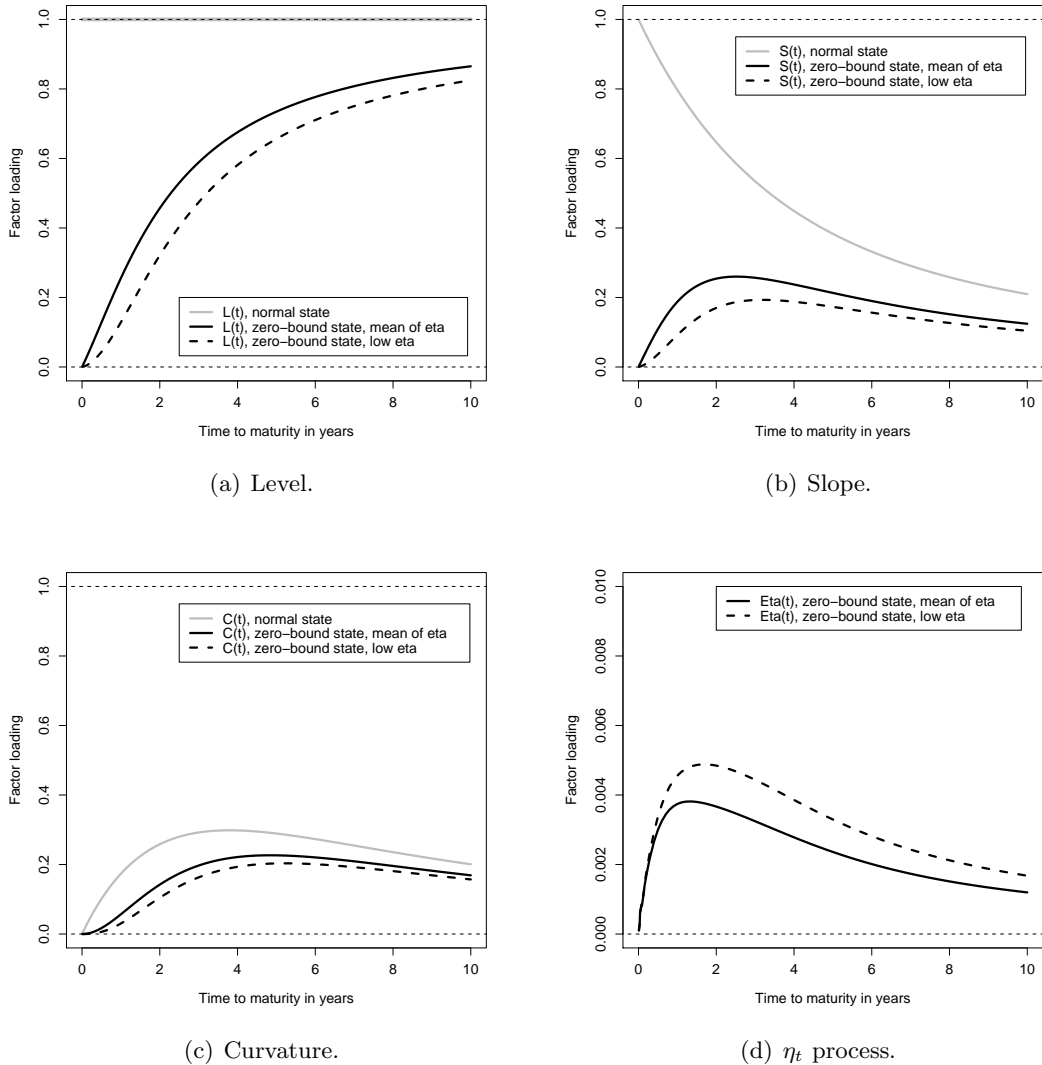


Figure 6: **Factor Loadings in Yield Function.** Illustration of the factor loadings in the zero coupon bond yield function. For the level, slope, and curvature factors both the normal and the zero-bound state loadings are shown. For the zero-bound state, loadings are shown both assuming the estimated average value of η_t as well as a low value of $\eta_t = 0.05$, while the three other state variables are fixed at their full sample averages. The parameters used in the calculations are those estimated on the full sample covering the period from January 4, 1985, to December 27, 2013.

Figure 6 shows the factor loadings of the state variables in the zero-coupon bond yield function in the zero-bound state and compares them to those in the normal state.²⁴ First, we note the significant drop in the sensitivity of short-term yields to variation in the level factor, which is more pronounced the lower the value of η_t . Second, the slope factor has a factor

reversion matrix K^P in either the standard or the regime-switching model.

²⁴As the zero-coupon bond yield function is nonlinear in the zero-bound state, the shown factor loadings are calculated as first-order approximations with the first three state variables fixed at their full sample averages, while η_t takes on two different values (see the caption of the figure for details).

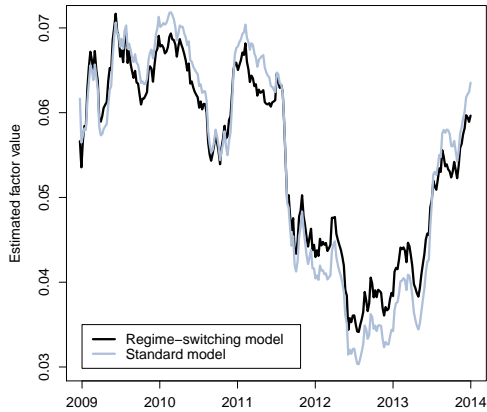
loading across maturities very similar to that of a curvature factor, which largely reflects the fact that the slope factor has no role to play for the shortest yield maturities in the zero-bound state. Again, this effect is more pronounced the lower the value of η_t , as an exit to the normal state is less likely. Third, and maybe not surprisingly, the curvature factor preserves a factor loading close to that of the normal state and is not very sensitive to variations in η_t . Finally, Figure 6(d) shows the factor loading of η_t . It exhibits a hump-shaped pattern, which is more pronounced the lower the value of η_t , with a peak near the one- to two-year maturity. When η_t is low, the economy is likely to remain in the zero-bound state for longer. As a consequence, bond yields become more sensitive to news about η_t .

Figure 7 illustrates the estimated paths of the four state variables over the part of the sample that covers the zero-bound period. Note that for the first three factors (level, slope, and curvature), the results are compared to those we get from estimating the normal-state three-factor AFNS model on the full sample without imposing any regime switch. As shown in Figure 7(a), the level factor is little affected by the incorporation of the regime switch. Intuitively, if the economy is expected to return to the normal state in the foreseeable future, there should not be a sizeable wedge in long-term bond yields across the two regimes. Obviously, the slope factor is a different story. In the regime-switching model, this factor is systematically above the path from the standard model as shown in Figure 7(b) since it does not have to match the very low level of the shortest yields in the zero-bound state. To preserve the fit of medium-term yields, the higher path of the slope factor in the regime-switching model is offset by a slightly lower path for the curvature factor than in the standard model as illustrated in Figure 7(c). Despite these differences it should be noted that the time variation is very highly correlated across the two models for these three factors. Finally, as shown in Figure 7(d), the path of η_t is rather volatile with notable cycles around a general lower trend that is the result of the slow recovery after the financial crisis and the related downward revisions to the outlook for future monetary policy as I will discuss later.

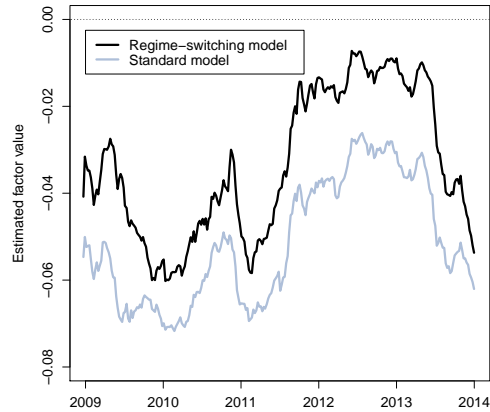
5 Model Performance Evaluation

In this section, I evaluate the performance of the regime-switching model in terms of fit, match to yield volatilities, and policy expectations. In doing so, I compare it to two established Gaussian models and a more recent shadow-rate model. The latter offers an alternative tractable way of modeling the asymmetric behavior of yields near the zero lower bound. Thus, this should provide a broad overall assessment of the strengths and weaknesses of the regime-switching model.

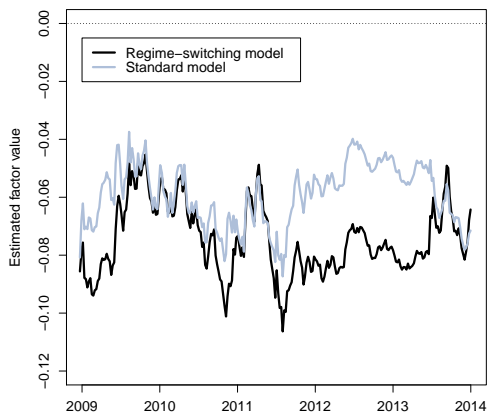
The first established model is the standard AFNS model favored by CR, denoted the CR model, while the other is the Kim and Wright (2005) model maintained at the Federal



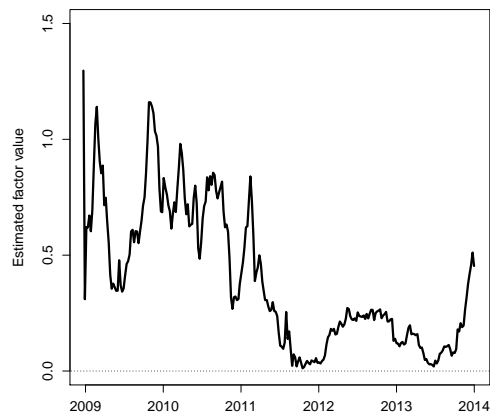
(a) Estimated level factors.



(b) Estimated slope factors.



(c) Estimated curvature factors.



(d) Estimated η_t process.

Figure 7: Estimated Factor Paths. Illustration of the estimated factor paths in the regime-switching model. For the level, slope, and curvature factors the results are compared to those of the standard three-factor AFNS model that preserves the normal state dynamics of the preferred regime-switching model specification throughout. The shown period covers the zero-bound state from December 19, 2008, to December 27, 2013, while the full sample used in model estimation covers the period from January 4, 1985, to December 27, 2013.

Reserve Board, denoted the KW model. Finally, I consider the shadow-rate model studied in Christensen and Rudebusch (2013).²⁵ Since this model is the shadow-rate equivalent of the CR model, I refer to it as the B-CR model.²⁶

²⁵To account for the zero lower bound, Black (1995) proposed using standard tools to model a shadow rate, s_t , that may be negative, while the observed short rate is truncated: $r_t = \max\{s_t, 0\}$. Krippner (2013b) provides an option-based approximation to Black’s shadow-rate concept, while Christensen and Rudebusch (2014) combine the latter with the AFNS model class to derive tractable shadow-rate AFNS models.

²⁶Following Kim and Singleton (2012), the prefix “B-” refers to a shadow-rate model in the spirit of Black (1995).

Maturity in months	Normal state					
	CR model		B-CR model		Regime-switching model	
	Mean	RMSE	Mean	RMSE	Mean	RMSE
3	-16.75	32.71	-17.28	32.71	-17.27	32.96
6	-5.92	15.64	-6.27	15.51	-6.19	15.72
12	0.00	0.00	-0.17	0.67	0.00	0.00
24	1.39	2.51	1.34	2.39	1.49	2.50
36	0.00	0.00	-0.02	0.09	0.00	0.00
60	-1.86	3.02	-1.88	2.81	-1.99	2.93
84	0.16	2.56	0.22	2.16	0.21	2.03
120	7.58	10.57	7.87	10.49	8.27	10.58

Maturity in months	Zero-bound state					
	CR model		B-CR model		Regime-switching model	
	Mean	RMSE	Mean	RMSE	Mean	RMSE
3	-16.75	21.23	-8.73	14.52	1.12	3.43
6	-9.47	11.94	-5.13	8.03	0.04	2.12
12	0.00	0.00	0.11	1.28	0.45	1.67
24	0.81	1.73	-0.65	1.39	-1.12	2.10
36	0.00	0.00	-0.31	0.61	0.54	1.75
60	-1.18	3.10	-0.53	2.10	0.13	0.72
84	0.16	3.57	-0.47	3.12	-0.41	1.44
120	4.52	11.12	1.34	7.42	1.83	4.81

Table 7: **Summary Statistics of Fitted Errors.** The mean fitted errors and the root mean squared fitted errors (RMSE) from the four-factor regime-switching model as well as those from the standard CR model and the shadow-rate B-CR model are shown. In each case, the summary statistics are calculated for two periods: (1) the normal state period from January 4, 1985, to December 12, 2008, and (2) the zero-bound state period from December 19, 2008, to December 27, 2013. The full sample used in each model estimation is weekly covering the period from January 4, 1985, to December 27, 2013. All numbers are measured in basis points.

5.1 Model Fit

Table 7 shows the summary statistics of the fitted errors from the regime-switching model introduced in this paper and those from the CR and B-CR models that preserve the same model dynamics throughout.²⁷ In each case, the summary statistics are calculated for two subsamples. The first is the normal state period that lasted until December 12, 2008, the other is the zero-bound state period from December 19, 2008, through 2013. We note that all three models underperform in fitting the short-term yields in the normal state. However, that is less critical when yields are far from the zero bound. On the contrary, once in the zero-bound state where three- and six-month yields have averaged 9 and 16 basis points, respectively, it is not satisfactory to have RMSEs for those two maturities on the order of 21 and 12 basis points, respectively, as in the CR model, and even the shadow-rate B-CR model

²⁷Summary data for the fit of the KW model is not available.

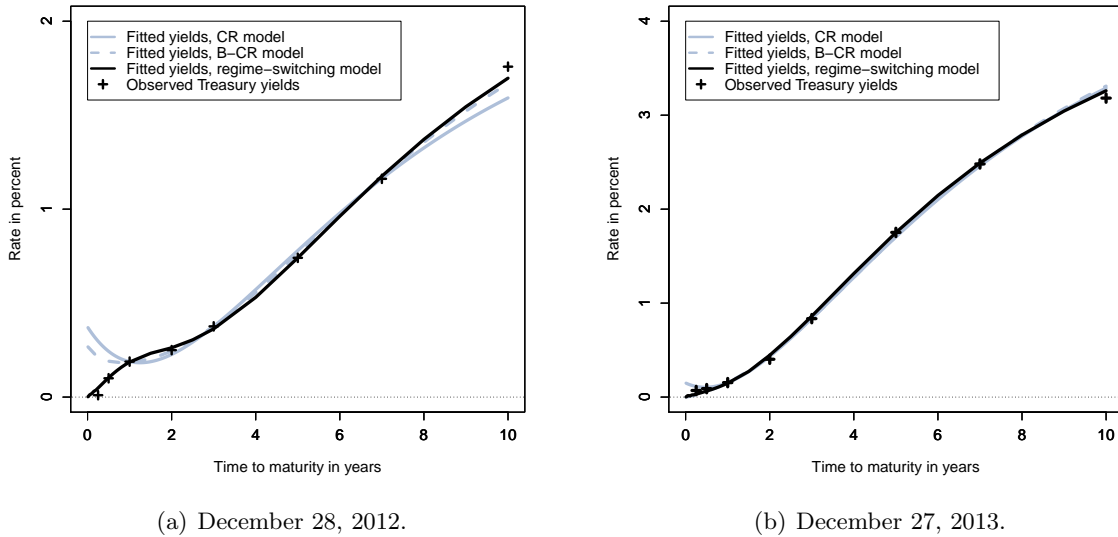


Figure 8: **Fitted Yield Curves.** Panel (a) shows the fitted yield curve as of December 28, 2012, from the regime-switching model as well as those from the standard CR model and the shadow-rate B-CR model. Panel (b) shows the corresponding results as of December 27, 2013.

produces RMSEs for those yields of 15 and 8 basis points, respectively. In contrast, for the regime-switching model, the introduction of the fourth factor with its unique characteristics is beneficial for the fit of yields in general, and short-term yields in particular. To better understand the difference in the results across the three models, Figure 8 shows the fitted yield curves from all three models as well as the observed yields on two dates, December 28, 2012, and December 27, 2013. On December 28, 2012, yields are particularly low and the term structure intriguing in its shape. The regime-switching model provides a very close fit to the entire term structure even on such days, while standard models, and even shadow-rate models, may have trouble matching the short end of the yield curve. On the other hand, when yields are not particularly low or the term structure is simple, as on December 27, 2013, all three models perform well and are hard to distinguish from each other.

5.2 Yield Volatility in the Zero-Bound State

In this section, I document that the regime-switching model produces notably lower short-term yield volatility in the zero-bound state as compared to the normal state. Also, I show that its implied yield volatility is closer to realized yield volatility measures than those implied by the shadow-rate B-CR model.²⁸

To provide evidence of the models' ability to match yield volatility near the zero lower bound, I compare their conditional one-month projection of yield volatility at various matu-

²⁸The CR and KW models are not included in this analysis due to their Gaussian nature.

rities to a measure of the subsequent 31-day realized yield volatilities.

In the normal state, where zero-coupon yields are affine functions of the state variables, the conditional predicted yield volatilities implied by the regime-switching are given by the square root of

$$V_t^P[y^N(T, T + \tau)] = \frac{1}{\tau^2} B^N(T, T + \tau)' V_t^P[X_T] B^N(T, T + \tau), \quad (6)$$

where $T - t$ is the prediction period, τ is the yield maturity, and $V_t^P[X_T]$ is the conditional covariance matrix. For affine diffusion processes, the latter is in general given by²⁹

$$V^P[X_T|X_t] = \int_t^T \exp(-K^P(T-s)) \Sigma D(E^P[X_s|X_t]) D(E^P[X_s|X_t])' \Sigma' \exp(-(K^P)'(T-s)) ds. \quad (7)$$

In the zero-bound state, where zero-coupon yields are nonlinear functions of the state variables, model-implied conditional predicted yield volatilities must be generated by simulation.³⁰

To evaluate the fit of these predicted one-month-ahead conditional yield standard deviations, I compare them to a standard measure of realized volatility based on the same data used in the model estimation, but at daily frequency. The realized standard deviation of the daily changes in the interest rates are generated for the 31-day period ahead on a rolling basis. The realized variance measure is used by Andersen and Benzoni (2010), Collin-Dufresne et al. (2009), and Jacobs and Karoui (2009) in their assessments of stochastic volatility models. For each observation date t the number of trading days N during the subsequent 31-day time window is determined (where N is most often 21 or 22) and the realized standard deviation is calculated as

$$RV_{t,\tau}^{STD} = \sqrt{\sum_{n=1}^N \Delta y_{t+n}^2(\tau)},$$

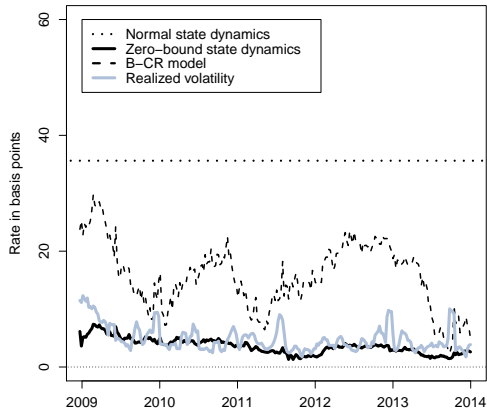
where $\Delta y_{t+n}(\tau)$ is the change in yield $y(\tau)$ from trading day $t + (n - 1)$ to trading day $t + n$.³¹

Figure 9 shows the results for four yield maturities: three-month, six-month, one-year, and two-year. In the normal state, the yields with two years or less to maturity have near identical conditional one-month yield volatilities of about 35 basis points, which are all constant due to the Gaussian dynamics. In the zero-bound state, the regime-switching model produces projected yield volatilities for short-term yields that closely match the corresponding subsequent yield volatility realizations. However, further out the yield curve the model

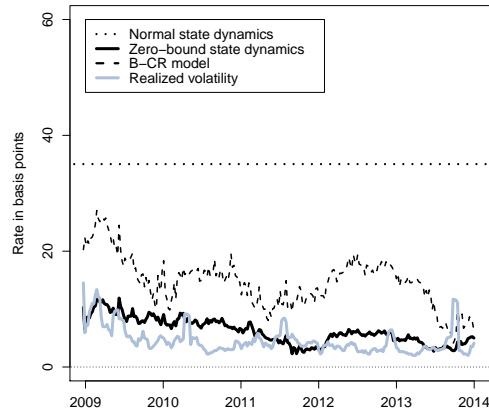
²⁹The conditional covariance matrix is calculated using the analytical solutions provided in Fisher and Gilles (1996).

³⁰Christensen and Rudebusch (2013) also use simulations to generate yield volatilities from the B-CR model.

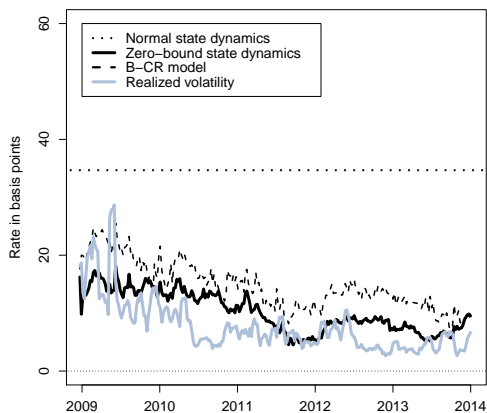
³¹Note that other measures of realized volatility have been used in the literature, such as the realized mean absolute deviation measure as well as fitted GARCH estimates. Collin-Dufresne et al. (2009) also use option-implied volatility as a measure of realized volatility.



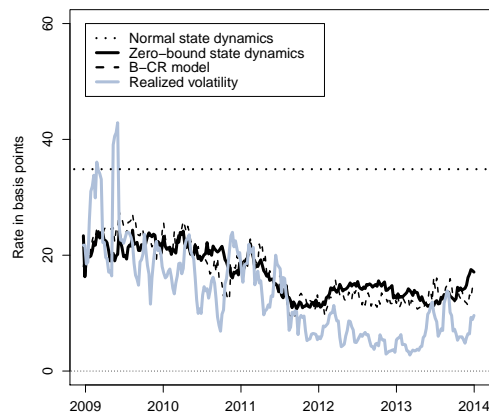
(a) Three-month yield.



(b) Six-month yield.



(c) One-year yield.



(d) Two-year yield.

Figure 9: One-Month Conditional Yield Volatilities. Illustration of the one-month conditional volatility of the three-month, six-month, one-year, and two-year Treasury yields implied by the regime-switching model using both its normal state and zero-bound state P -dynamics as well as those implied by the B-CR model. Also shown are the subsequent 31-day realized volatility series calculated based on daily data as described in the main text. The period shown covers the zero-bound state from December 19, 2008, to December 27, 2013, while the full sample used in model estimation covers the period from January 4, 1985, to December 27, 2013.

starts to approximate the normal state dynamics characterized by constant yield volatility. Still, the model continues to provide a fairly close fit to those realized yield volatility series. Furthermore, as can be seen in Figure 9(d), there remains a clear wedge between the normal state and zero-bound state yield volatility dynamics, even at the longer maturities.³² Finally,

³²Unreported results show that the fit of long-term yield volatilities can be improved through the incorporation of stochastic volatility into the Nelson-Siegel level factor as in Christensen et al. (2012). However, this is left for future refinement.

the comparison to the shadow-rate B-CR model suggests that the regime-switching model is competitive at matching the compression in volatility in the short end of the yield curve relative to that class of models.³³

5.3 Monetary Policy Expectations in the Zero-Bound State

The objective of this section is to assess the reasonableness of the monetary policy expectations implied by the regime-switching model. To do so, I compare them to those derived from the three alternative term structure models and to those implied by the rates on federal funds futures contracts.

In the zero-bound state, the expected short rate τ years ahead is given by³⁴

$$\begin{aligned} E_t^P[r_{t+\tau}] &= 0 \cdot E_t^P \left[e^{-\int_t^{t+\tau} \eta_u du} \right] + E_t^P \left[\int_t^{t+\tau} \eta_s e^{-\int_t^s \eta_u du} r_{t+\tau} ds \right] \\ &= \int_t^{t+\tau} E_t^P \left[\eta_s e^{-\int_t^s \eta_u du} E_s^P[r_{t+\tau}] \right] ds. \end{aligned}$$

Ideally, the regime-switching model’s accuracy in projecting future short rates should be tested in a real-time forecast exercise over many years like the ones performed by CR and Christensen and Rudebusch (2013). However, the limited data from the zero-bound state prevents such an exercise at the time of this writing. Instead, to assess the regime-switching model’s short-rate projections during the most recent period, I use the full-sample estimation results and compare the variation in the one- and two-year short rate forecasts from the regime-switching model to the corresponding results from the CR, B-CR, and KW models, and to the rates on one- and two-year federal funds futures contracts, all shown in Figure 10.³⁵ In doing so, it should be emphasized that the existence of time-varying risk premiums, even in very short-term federal funds futures contracts, is well documented (see Piazzesi and Swanson 2008). However, the size of risk premiums in such short-term contracts are presumably small relative to the sizeable variation observed during the time period shown in Figure 10. As a consequence, I interpret the bulk of the variation from 2007 to 2009 as reflecting declines in short rate expectations. Furthermore, since August 2011, most evidence—including the one shown in Figure 11 below—suggests that risk premiums have been significantly depressed, likely to a point that the zero-risk-premium assumption for the futures contracts applied here may provide a satisfactory approximation. Combined, these observations suggest that it is

³³Using a 91-day window leads to the same conclusion. Results are available upon request.

³⁴Appendix B describes the calculation of these expectations.

³⁵The futures data are from Bloomberg. The one-year futures rate is the weighted average of the rates on the 12- and 13-month federal funds futures contracts, while the two-year futures rate is the rate on the 24-month federal funds futures contract through 2010, and the weighted average of the rates on the 24- and 25-month contracts since then. Absence of data on the 24-month contracts prior to 2007 determines the start date for the analysis.

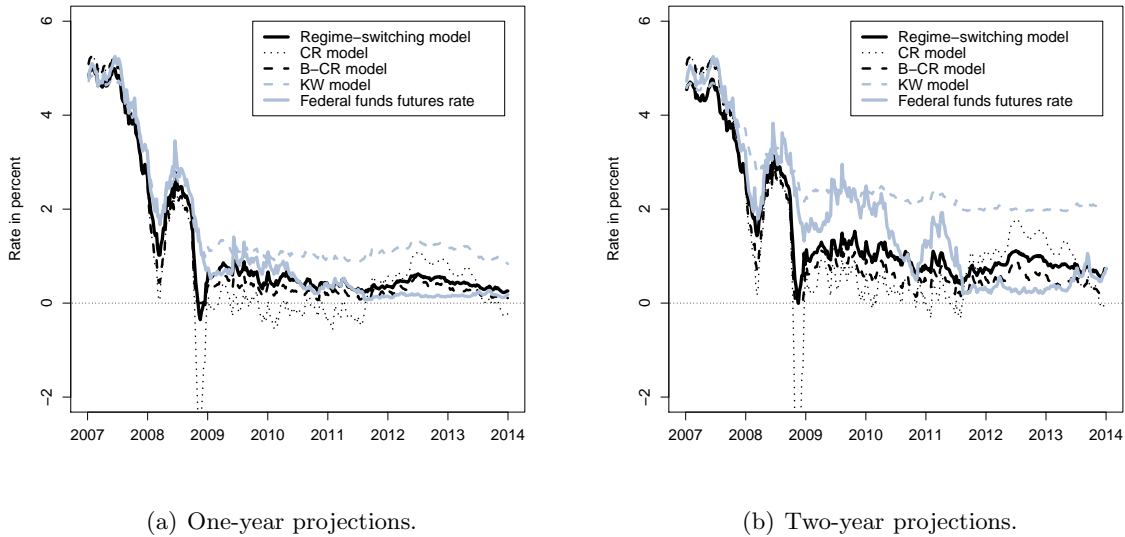


Figure 10: **Short Rate Projections.**

Panel (a) illustrates the one-year short rate projections from the regime-switching, CR, B-CR, and KW models with a comparison to the rates on one-year federal funds futures. Panel (b) shows the corresponding results for a two-year projection period with a comparison to the rates on two-year federal funds futures. The data are weekly covering the period from January 5, 2007, to December 27, 2013.

defensible for most of the shown seven-year period to map the models' short rate projections to the rates on the federal funds futures contracts *without* adjusting them for risk premiums.

At the one-year and two-year forecast horizons, the correlations between short rate forecasts from the CR model and the federal funds futures rates are 88.6% and 68.6%, respectively. For the KW model, the correlations are 97.7% and 95.1%, respectively, while the policy rate projections from the B-CR model have correlations with the futures rates equal to 96.9% and 90.3%, respectively. For the regime-switching model, these correlations are 97.7% and 91.1%, respectively. Thus, as measured by correlations, the performance is very similar across models, maybe with the exception of the CR model.

If, instead, a distance metric is used, the results are quite different and more differential. Table 8 reports the mean differences and the root mean squared differences (RMSD) from all four models relative to the rates of the federal funds futures contracts. We note that the two standard models are not particularly close to the futures rates either on average or as measured by RMSDs. Thus, they do not appear to be well placed to provide accurate estimates of the changes in investors' short- to medium-term expectations for future monetary policy, while the economy is in the zero-bound state. On the other hand, we do see the shadow-rate B-CR model deliver significant improvement in accuracy of the estimated policy expectations, consistent with the findings of Christensen and Rudebusch (2013). Finally, and

Model	One-year contract		Two-year contract	
	Mean	RMSD	Mean	RMSD
Regime-switching model	-6.55	34.62	-24.71	65.16
CR model	-33.50	83.79	-50.89	131.68
B-CR model	-20.69	43.21	-47.39	79.07
KW model	46.89	65.71	85.00	110.75

Table 8: **Summary Statistics of Differences relative to Federal Funds Futures Rates.** The mean differences and the root mean squared differences (RMSD) between the short rate expectations from four term structure models, on one side, and federal funds futures rates, on the other, are reported for two contract horizons. In each case, the summary statistics are calculated for the periods from January 3, 2007, to December 27, 2013. All numbers are measured in basis points.

most importantly, it is noted that the regime-switching model stands out, in that it delivers the smallest mean differences and RMSDs at both contract horizons. Based on this evidence, I conclude that the regime-switching model delivers projections for future monetary policy that appear to be at least as accurate as those from any of the alternative models considered.

5.4 Term Premiums in the Zero-Bound State

In this section, I first describe how long-term yields are decomposed into policy expectations and term premium components within the regime-switching model before proceeding to a comparison to the three alternative models.

In general, the term premium component in the yield of a zero-coupon bond with maturity in τ years is defined as

$$TP_t(\tau) = y(t, t + \tau) - \frac{1}{\tau} \int_t^{t+\tau} E_t^P[r_s] ds$$

and reflects the difference between the long-term yield that can be settled today and the expected return from a rollover strategy that earns the risk-free rate.³⁶

In the normal state, the term premium takes its usual form

$$TP_t^N(\tau) = y^N(t, t + \tau) - \frac{1}{\tau} \int_t^{t+\tau} E_t^P[r_s] ds,$$

where the instantaneous short rate is the sum of the first two factors

$$r_t = L_t + S_t.$$

³⁶Note that a Jensen's inequality term has been left out for the rollover strategy in this definition.

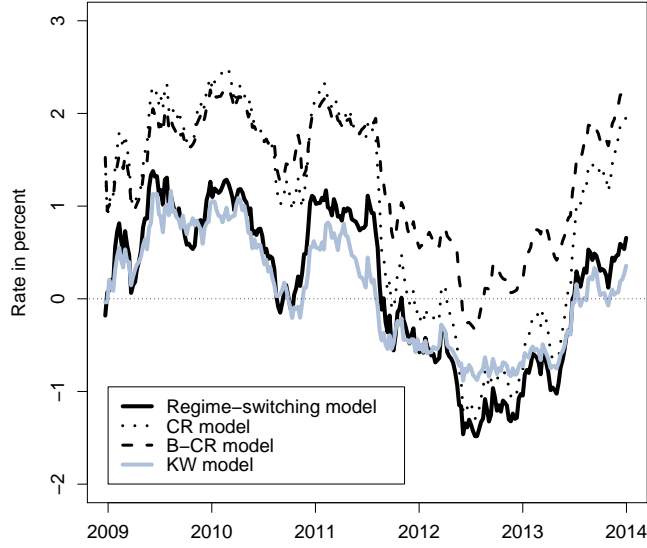


Figure 11: **Estimated Ten-Year Term Premiums.** Illustration of the estimated ten-year zero-coupon term premium from the regime-switching model with a comparison to the corresponding estimates from the CR, B-CR, and KW models. The data shown cover the period from December 19, 2008, to December 27, 2013.

In the zero-bound state, the formula for the term premium is given by³⁷

$$\begin{aligned}
 TP_t^Z(\tau) &= y^Z(t, t + \tau) - \frac{1}{\tau} \left(0 \cdot E_t^P [e^{-\int_t^{t+\tau} \eta_u du}] + E_t^P \left[\int_t^{t+\tau} \eta_s e^{-\int_t^s \eta_u du} \int_s^{t+\tau} r_u du ds \right] \right) \\
 &= y^Z(t, t + \tau) - \frac{1}{\tau} \int_t^{t+\tau} E_t^P \left[\eta_s e^{-\int_t^s \eta_u du} E_s^P \left[\int_s^{t+\tau} r_u du \right] \right] ds.
 \end{aligned}$$

The results for the ten-year term premium since late 2008 are illustrated in Figure 11. It is noted that all four models broadly paint a similar picture. From early 2009 through 2010 and most of 2011, term premiums were elevated before dropping significantly towards the end of that year after the Fed provided explicit policy forward guidance for the first time at the August 2011 FOMC meeting and started its maturity extension program, or “twist”, at the September 2011 FOMC meeting.³⁸ Between then and the first half of 2013, a combination of forward guidance and asset purchases by the Fed kept term premiums at historically low levels. Finally, during the summer of 2013, markets reacted strongly in anticipation of the

³⁷Appendix C shows how term premiums are calculated in both the normal state and the zero-bound state.

³⁸This program operated from September 2011 through 2012 and involved purchases of more than \$600 billion of long-term Treasury securities (defined as bonds with more than six years to maturity) financed by selling an equal amount of shorter-term Treasuries (defined as bonds with less than three years to maturity). See Cahill et al. (2013) and Li and Wei (2013) for analysis.

Correlation	Ten-year term premiums			
	RS model	CR model	B-CR model	KW model
RS model	1	0.987	0.960	0.957
CR model		1	0.977	0.953
B-CR model			1	0.896
KW model				1

Table 9: **Pairwise Correlations of Term Premiums.** The table contains the pairwise correlations between the ten-year term premiums from the regime-switching (RS) model, the CR model, the B-CR model, and the KW model. The sample is weekly from December 19, 2008, to December 27, 2013.

first decision to reduce or taper the open-ended asset purchases that were on-going at the time.³⁹ The similarity in time variation is confirmed in Table 9, which reports the correlations between all four ten-year term premium series since late 2008 that are indeed all very high. However, Figure 11 also indicates that there is a notable difference in levels most of the time between the estimates from the CR and B-CR models, on one side, and those from the regime-switching and KW models, on the other. This difference can be traced back to a level difference in the projected paths for future short rates at medium- to long-term horizons, where in particular the B-CR model indicates a very slow normalization of monetary policy.

6 The Exit from the Zero-Bound State

In this section, I analyze the model-implied distribution of the exit time from the zero-bound state that is unique to the regime-switching model presented in this paper.⁴⁰

The estimated probability of remaining in the zero-bound state is given by

$$E_t^P \left[e^{-\int_t^T \eta_u du} \right] = \exp \left(A_\eta^P(t, T) + B_\eta^P(t, T)\eta_t \right), \quad (8)$$

while the continuous intensity of exiting the zero-bound state is

$$E_t^P \left[\eta_T e^{-\int_t^T \eta_u du} \right] = \exp \left(A_\eta^P(t, T) + B_\eta^P(t, T)\eta_t \right) \times \left[C_\eta^P(t, T) + D_\eta^P(t, T)\eta_t \right], \quad (9)$$

³⁹The Fed's third asset purchase program (QE3) was launched in September 2012 and at first only involved purchases of mortgage-backed securities (MBS) at a monthly pace of \$40 billion. In December 2012, the program was expanded to include purchases of Treasury securities at a monthly pace of \$45 billion. In December 2013, the Fed started the process of gradually tapering down the asset purchases. However, throughout, the QE3 program was open ended, in that no specific end date was provided for the program.

⁴⁰Bauer and Rudebusch (2014) use shadow-rate models to assess the time of exit, while Monfort et al. (2014) construct a novel affine term structure model that also delivers exit time distributions.

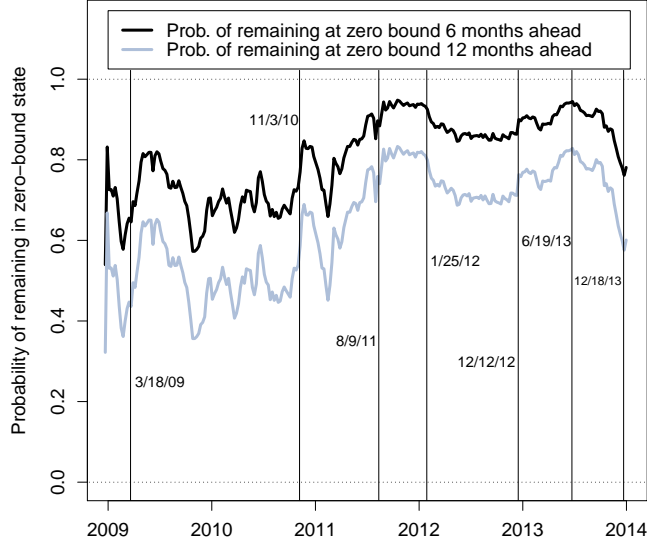


Figure 12: **Probability of Remaining in the Zero-Bound State.** Illustration of the estimated probability of remaining in the zero-bound state six and twelve months ahead. The sample used in model estimation consists of weekly U.S. Treasury zero-coupon bond yields covering the period from January 4, 1985, to December 27, 2013.

where⁴¹

$$\begin{aligned}
 A_{\eta}^P(t, T) &= \frac{2\kappa_{44}^P \theta_4^P}{\sigma_{\eta}^2} \ln \left[\frac{2\phi_{\eta}^P e^{\frac{1}{2}(\phi_{\eta}^P + \kappa_{44}^P)(T-t)}}{2\phi_{\eta}^P + (\phi_{\eta}^P + \kappa_{44}^P)(e^{\phi_{\eta}^P(T-t)} - 1)} \right], \\
 B_{\eta}^P(t, T) &= \frac{-2(e^{\phi_{\eta}^P(T-t)} - 1)}{2\phi_{\eta}^P + (\phi_{\eta}^P + \kappa_{44}^P)[e^{\phi_{\eta}^P(T-t)} - 1]}, \\
 C_{\eta}^P(t, T) &= 2\kappa_{44}^P \theta_4^P \frac{e^{\phi_{\eta}^P(T-t)} - 1}{2\phi_{\eta}^P + (\phi_{\eta}^P + \kappa_{44}^P)(e^{\phi_{\eta}^P(T-t)} - 1)}, \\
 D_{\eta}^P(t, T) &= \frac{4(\phi_{\eta}^P)^2 e^{\phi_{\eta}^P(T-t)}}{[2\phi_{\eta}^P + (\phi_{\eta}^P + \kappa_{44}^P)(e^{\phi_{\eta}^P(T-t)} - 1)]^2}
 \end{aligned}$$

with

$$\phi_{\eta}^P = \sqrt{(\kappa_{44}^P)^2 + 2\sigma_{\eta}^2}.$$

The estimated probability of remaining in the zero-bound state is illustrated in Figure 12 at the six- and twelve-month forecast horizon. Also, included are seven key dates with

⁴¹These results are obtained by combining the P -dynamics of the η_t -process with analytical formulas provided in Christensen (2007).

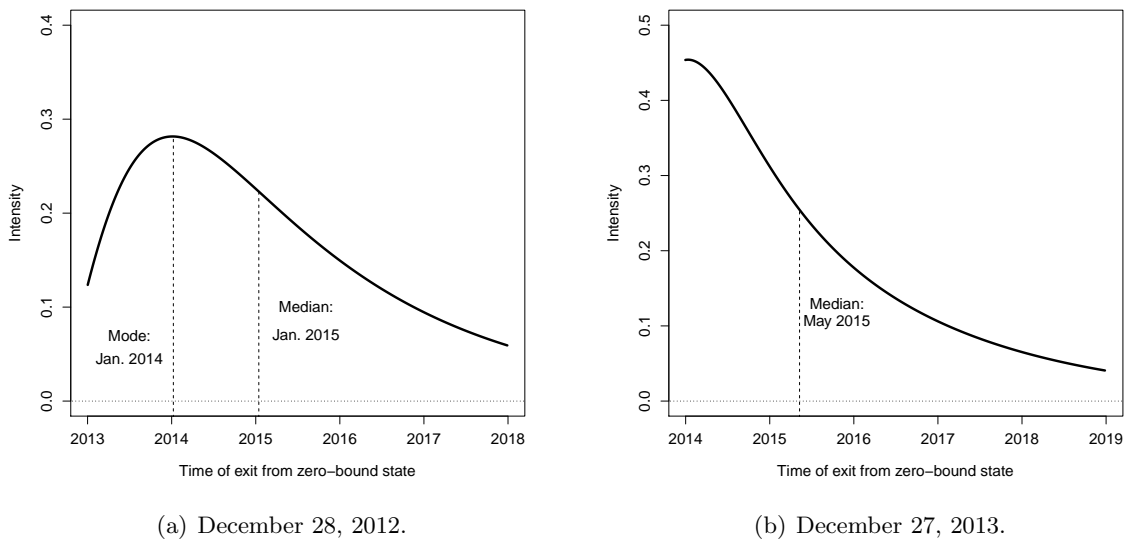


Figure 13: **Distribution of the Exit Time from the Zero-Bound State.** Panel (a) shows the continuous intensity of exiting the zero-bound state as of December 28, 2012. Vertical dashed lines indicate both the mode and the median of the exit time distribution. Panel (b) shows the continuous intensity of exiting the zero-bound state as of December 27, 2013. A vertical line indicate the median of the exit time distribution.

major decisions by the FOMC regarding either its LSAP programs or its forward guidance for future policy. For the announcements until spring 2013, there are notable upward spikes in the estimated probability of remaining at the zero bound in the weeks after each announcement. The extension of the forward guidance at the January 2012 FOMC meeting is the notable exception. This suggests that part of the effect from unconventional policies comes from a signaling channel through which the FOMC policy actions are interpreted to indicate that the policy rate will remain at its lower bound longer, as also emphasized by Bauer and Rudebusch (2013) and CR. Consistent with this interpretation, the probability of remaining in the zero-bound state declined in the period after the June 2013 FOMC meeting when then-Chairman Bernanke indicated that the FOMC would soon taper its asset purchases. Clearly, investors saw it as an indication that the zero-interest rate policy might come to an end more quickly than previously anticipated. Finally, as a consequence of investors' forward looking behavior, the actual announcement of the tapering decision at the December 2013 FOMC meeting only generated a modest additional reaction.⁴²

Figure 13 shows the continuous intensity of the exit time distribution on two recent dates, December 28, 2012, and December 27, 2013. It is noted that both distributions are heavily skewed to the right. On December 28, 2012, when the probability of remaining in the zero-bound state was high, the mode and the median exit time are located in the future. On the

⁴²See Christensen (2014) for further discussion.

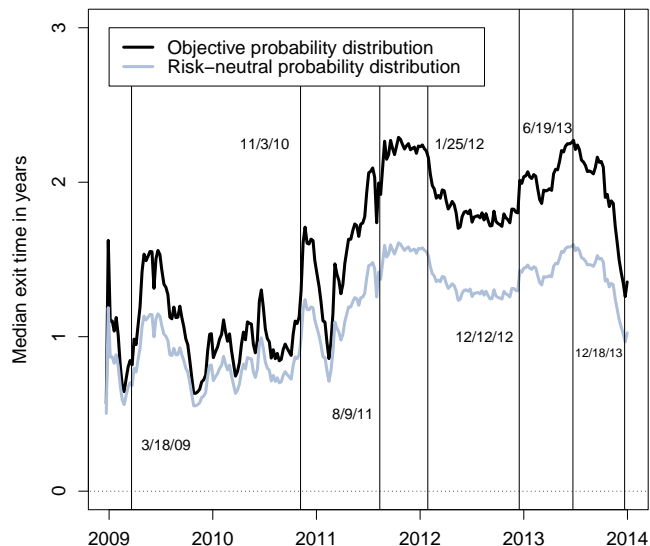


Figure 14: **Median Exit Time from the Zero-Bound State.** Illustration of the estimated median exit time from the zero-bound state under both the objective P probability measure and the risk-neutral Q probability measure from December 19, 2008, to December 27, 2013.

other hand, on December 27, 2013, the probability of remaining in the zero-bound state was much lower. As a result, the exit time distribution is less heavily skewed and the mode is for an immediate exit to the normal state. Since the distributions are heavily skewed, the mode is not the appropriate statistic to describe the exit time distribution, even though it obviously indicates the most likely single exit date. Instead, I focus on the median exit time, that is, the exit time that splits the probability mass in half. These dates are indicated with vertical dashed lines in Figures 13(a) and 13(b). As of December 27, 2013, the median exit time is located in May 2015.

The variation in the estimated median exit time from the zero-bound state since December 19, 2008, is shown in Figure 14. Also shown is the risk-neutral median exit time calculated based on the model's Q -dynamics used for pricing. As in Figure 12, most key FOMC announcements during the shown period had significant effects on the median exit time. Furthermore, it is noted that the priced median exit time calculated using the risk-neutral Q -dynamics is always shorter than the objective median exit time, but with varying difference. This suggests that the risk of exiting the zero-bound state carries a notable time-varying premium, which is higher when it is more likely for the economy to remain in the zero-bound state as it would be particularly costly for bond holders to be wrong in projecting a continuation of the zero-bound state under those circumstances.

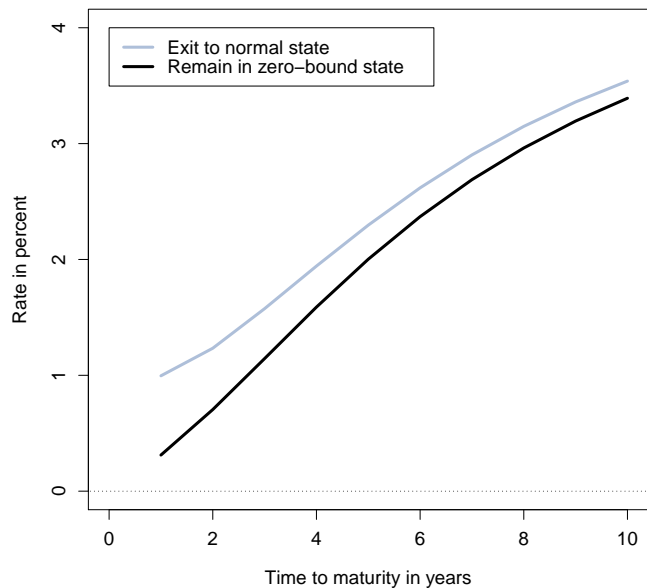


Figure 15: **Forecasted Yield Curves One Year Ahead.** Illustration of the forecasted yield curves one year ahead as of December 27, 2013, contingent on whether the economy remains in the zero-bound state or exits to the normal state.

6.1 Yield Curve Projections

As a final exercise, I use the regime-switching model to forecast the yield curve one year ahead as of the end of the sample depending on whether the economy remains in the zero-bound state or manages to exit to the normal state before the end of the forecast horizon.

Figure 15 illustrates the result of this exercise. Contingent on the economy exiting to the normal state over the forecast horizon, the one- and two-year yields would be 68 and 53 basis points higher than otherwise, respectively, while the wedge between the outcome-contingent forecasts of long-term yields is much smaller as investors expect the economy to exit at some point before the maturity of those bonds. This type of forecast exercise could be useful for risk management purposes. Alternatively, it could be used to stress test banks' portfolios as part of assessing their capital adequacy while in the zero-bound state.

7 Conclusion

In this paper, I extend the existing literature on regime-switching models of the yield curve by modifying a standard three-factor term structure model to account for the special dynamics of the Treasury yield curve when the monetary policy instrument is at its effective zero bound. Specifically, I introduce an additional regime referred to as the zero-bound state in which

the instantaneous risk-free rate is constant at zero. The novel feature of the model is that the probability of returning to the normal state is allowed to be time-varying under both the objective and the risk-neutral probability measures.

The highlight of the model is that it delivers estimates of the time-varying probability of the economy leaving the zero-bound state within any relevant forecast horizon. Also, the model provides outcome-contingent forecasts of future yield curves depending on whether the economy remains in the zero-bound state or exits to the normal state during the forecast period. This could be useful for stress tests of bond portfolios and for portfolio risk management in general while in the zero-bound state. Finally, the model is arbitrage-free, tractable, provides a good fit, delivers reasonable projections for future short rates, and matches the compression of short-term yield volatilities since 2009.

The results show that during the 2009-2012 period the exit probabilities generally declined, consistent with the efforts by the FOMC to provide more monetary stimulus to support the tepid recovery. Furthermore, the yield curve projections at the end of the sample suggest that, in the event of an exit to the normal state over the following year, one- and two-year yields would be 68 and 53 basis points higher than otherwise, respectively, while the ten-year yield would show much more modest increases as markets have already priced a high probability that the U.S. economy will return to the normal state before its maturity, making the specific timing of the regime switch less relevant for such long-term yields.

It is prudent to note that the model does not impose a zero lower boundary for the model-implied bond yields. However, this could be obtained by incorporating stochastic volatility into the three state variables in the normal state along the lines of Christensen et al. (2014). Such refinements are left for future research.

Appendix A: Kalman Filter Estimation of the Regime-Switching Model

The estimation of the regime-switching model is based on the Kalman filter, but is nonstandard for two reasons. First, we need to handle the switch to the zero-bound state in mid-December 2008. Second, once the economy is in the zero-bound state, zero-coupon bond yields are no longer affine functions of the state variables and the fourth state variable has non-Gaussian dynamics. For a start, though, it is important to note that, in the normal state, the model is Gaussian and identical to the AFNS models introduced in CDR. Hence, for that part of the sample, the Kalman filter algorithm proceeds as described in CDR and repeated here for convenience in order to detail the adjustments needed to do filtering in the zero-bound state.

For the affine Gaussian models, in general, the conditional mean vector and the conditional covariance matrix are

$$\begin{aligned} E^P[X_T|\mathcal{F}_t] &= (I - \exp(-K^P \Delta t))\theta^P + \exp(-K^P \Delta t)X_t, \\ V^P[X_T|\mathcal{F}_t] &= \int_0^{\Delta t} e^{-K^P s} \Sigma \Sigma' e^{-(K^P)' s} ds, \end{aligned}$$

where $\Delta t = T - t$. We compute conditional moments of discrete observations and obtain the state transition equation

$$X_t = (I - \exp(-K^P \Delta t))\theta^P + \exp(-K^P \Delta t)X_{t-1} + \xi_t,$$

where Δt is the time between observations. The measurement equation is (see equation (1))

$$y_t = A + BX_t + \varepsilon_t.$$

The assumed error structure is

$$\begin{pmatrix} \xi_t \\ \varepsilon_t \end{pmatrix} \sim N \left[\begin{pmatrix} 0 \\ 0 \end{pmatrix}, \begin{pmatrix} Q & 0 \\ 0 & H \end{pmatrix} \right],$$

where the matrix H is assumed diagonal, while the matrix Q has the following structure⁴³

$$Q = \int_0^{\Delta t} e^{-K^P s} \Sigma \Sigma' e^{-(K^P)' s} ds.$$

In addition, the transition and measurement errors are assumed orthogonal to the initial state.

Now consider Kalman filtering, which is used to evaluate the likelihood function.

Due to the assumed stationarity, the filter is initialized at the unconditional mean and variance of the state variables under the P -measure: $X_0 = \theta^P$ and $\Sigma_0 = \int_0^{\infty} e^{-K^P s} \Sigma \Sigma' e^{-(K^P)' s} ds$.

Denote the information available at time t by $Y_t = (y_1, y_2, \dots, y_t)$, and denote model parameters by ψ . Consider period $t - 1$ and suppose that the state update X_{t-1} and its mean square error matrix Σ_{t-1} have been obtained. The prediction step is

$$X_{t|t-1} = E^P[X_t|Y_{t-1}] = \Phi_t^{X,0}(\psi) + \Phi_t^{X,1}(\psi)X_{t-1},$$

$$\Sigma_{t|t-1} = \Phi_t^{X,1}(\psi)\Sigma_{t-1}\Phi_t^{X,1}(\psi)' + Q_t(\psi),$$

where $\Phi_t^{X,0} = (I - \exp(-K^P \Delta t))\theta^P$, $\Phi_t^{X,1} = \exp(-K^P \Delta t)$, and $Q_t = \int_0^{\Delta t} e^{-K^P s} \Sigma \Sigma' e^{-(K^P)' s} ds$, while Δt is the time between observations.

⁴³Throughout, conditional and unconditional covariance matrices are calculated using the analytical solutions provided in Fisher and Gilles (1996).

In the time- t update step, $X_{t|t-1}$ is improved by using the additional information contained in Y_t :

$$X_t = E[X_t|Y_t] = X_{t|t-1} + \Sigma_{t|t-1}B(\psi)'F_t^{-1}v_t,$$

$$\Sigma_t = \Sigma_{t|t-1} - \Sigma_{t|t-1}B(\psi)'F_t^{-1}B(\psi)\Sigma_{t|t-1},$$

where

$$v_t = y_t - E[y_t|Y_{t-1}] = y_t - A(\psi) - B(\psi)X_{t|t-1},$$

$$F_t = \text{cov}(v_t) = B(\psi)\Sigma_{t|t-1}B(\psi)' + H(\psi),$$

$$H(\psi) = \text{diag}(\sigma_\varepsilon^2(\tau_1), \dots, \sigma_\varepsilon^2(\tau_N)).$$

At this point, the Kalman filter has delivered all ingredients needed to evaluate the Gaussian log likelihood, the prediction-error decomposition of which is

$$\log l(y_1, \dots, y_T; \psi) = \sum_{t=1}^T \left(-\frac{N}{2} \log(2\pi) - \frac{1}{2} \log |F_t| - \frac{1}{2} v_t' F_t^{-1} v_t \right),$$

where N is the number of observed yields. Now, the likelihood is numerically maximized with respect to ψ using the Nelder-Mead simplex algorithm. Upon convergence, the standard errors are obtained from the estimated covariance matrix,

$$\widehat{\Omega}(\widehat{\psi}) = \frac{1}{T} \left[\frac{1}{T} \sum_{t=1}^T \frac{\partial \log l_t(\widehat{\psi})}{\partial \psi} \frac{\partial \log l_t(\widehat{\psi})'}{\partial \psi} \right]^{-1},$$

where $\widehat{\psi}$ denotes the estimated model parameters.

The introduction of stochastic volatility in the zero-bound state implies that the factors are no longer simply Gaussian for that part of the sample. The way to proceed is to simply approximate the true probability distribution of the state variables with the first and second moments and use the Kalman filter algorithm *as if* the state variables were Gaussian.⁴⁴ Thus, the state equation continues to be given by

$$X_t = (I - \exp(-K^P \Delta t))\theta^P + \exp(-K^P \Delta t)X_{t-1} + \xi_t, \quad \xi_t \sim N(0, V_{t-1}),$$

while the conditional covariance matrix for affine diffusion processes with stochastic volatility is given by

$$V^P[X_T|X_t] = \int_t^T \exp(-K^P(T-s))\Sigma D(E^P[X_s|X_t])D(E^P[X_s|X_t])'\Sigma' \exp(-(K^P)'(T-s))ds.$$

In handling the switch date to the zero-bound state, the approach of Christensen et al. (2010) is followed. For the first 24 years of the sample when the economy is in the normal state, $e^{-K^P \Delta t}$, $(I - e^{-K^P \Delta t})\theta^P$, and the conditional covariance matrix

$$V^P[X_T|\mathcal{F}_t] = \int_0^{\Delta t} e^{-K^P s} \Sigma \Sigma' e^{-(K^P)' s} ds$$

are calculated using the upper 3×3 part of K^P and the upper 3×1 part of θ^P . Once the economy hits the zero bound on December 16, 2008, the θ^P , K^P and Σ used in the Kalman filter algorithm represent the full

⁴⁴A few notable examples of papers that follow this approach include Duffee (1999), Driessen (2005), and Feldhütter and Lando (2008).

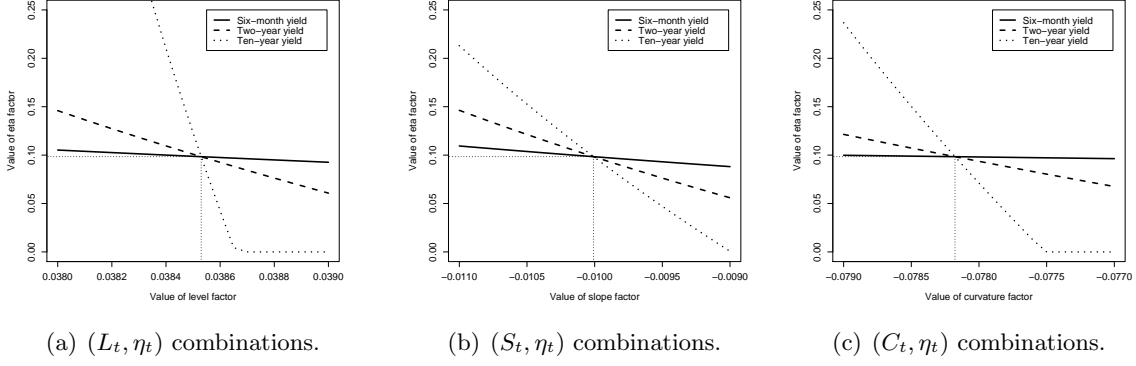


Figure 16: **Linearity of Yield Function in the Zero-Bound State.** Illustration of the combinations of (L_t, η_t) , (S_t, η_t) , and (C_t, η_t) that deliver a perfect fit to the six-month, two-year, and ten-year Treasury yields implied by the regime-switching model as of December 28, 2012.

four-dimensional dynamics of the state variables and the conditional covariance matrix is calculated as⁴⁵

$$\int_t^{t+\tau} e^{-K^P(t+\tau-s)} \Sigma D(E^P[X_s|X_t]) D(E^P[X_s|X_t])' \Sigma' e^{-(K^P)'(t+\tau-s)} ds.$$

Furthermore, in the zero-bound state, we need to use the extended Kalman filter because the zero-coupon bond yields are no longer affine functions of the state variables. Instead, the measurement equation takes the general form

$$y_t^Z = z(X_t; \psi) + \varepsilon_t^Z.$$

In the extended Kalman filter, this equation is linearized using a first-order Taylor expansion around the best guess of X_t in the prediction step of the Kalman filter algorithm. Thus, in the notation introduced above, this best guess is denoted $X_{t|t-1}$ and the approximation is given by

$$z(X_t; \psi) \approx z(X_{t|t-1}; \psi) + \left. \frac{\partial z(X_t; \psi)}{\partial X_t} \right|_{X_t=X_{t|t-1}} (X_t - X_{t|t-1}).$$

Thus, by defining

$$A_t(\psi) \equiv z(X_{t|t-1}; \psi) - \left. \frac{\partial z(X_t; \psi)}{\partial X_t} \right|_{X_t=X_{t|t-1}} X_{t|t-1}, B_t(\psi) \equiv \left. \frac{\partial z(X_t; \psi)}{\partial X_t} \right|_{X_t=X_{t|t-1}},$$

the measurement equation can be given on an affine form as

$$y_t^Z = A_t(\psi) + B_t(\psi)X_t + \varepsilon_t^Z$$

and the steps in the algorithm proceed as previously described.

Figure 16 demonstrates that the bond yield function in the zero-bound state is close to linear locally even in the η_t -dimension. This suggests that the approximation error of the extended Kalman filter is likely to be minuscule.

Finally, in the empirical implementation, the measurement error distribution is assumed to switch as well. Hence, both an H^N and H^Z matrix, each with eight $\sigma_\varepsilon^2(\tau_i)$ parameters, are estimated to account for the difference in the size of the fitted errors across the two regimes.

⁴⁵Once the economy exits the zero-bound state, the change in the transition equation is simply reversed.

Appendix B: Policy Expectations in the Regime-Switching Model

In the normal state, the instantaneous short rate is the sum of the first two factors

$$r_t = L_t + S_t.$$

Neglecting the small chance of switching to the zero-bound state, the conditional mean of the state variables can be calculated as

$$E^P[X_{t+\tau}|\mathcal{F}_t] = (I - \exp(-K^P \tau))\theta^P + \exp(-K^P \tau)X_t,$$

where, in general,

$$K^P = \begin{pmatrix} \kappa_{11}^P & \kappa_{12}^P & \kappa_{13}^P \\ \kappa_{21}^P & \kappa_{22}^P & \kappa_{23}^P \\ \kappa_{31}^P & \kappa_{32}^P & \kappa_{33}^P \end{pmatrix} \quad \text{and} \quad \theta^P = \begin{pmatrix} \theta_1^P \\ \theta_2^P \\ \theta_3^P \end{pmatrix}.$$

Thus, the conditional mean of the instantaneous short rate is given by

$$E_t^P[r_{t+\tau}] = E_t^P[L_{t+\tau}] + E_t^P[S_{t+\tau}].$$

In the zero-bound state, the expected instantaneous short rate τ years ahead is given by

$$E_t^P[r_{t+\tau}] = 0 \cdot E_t^P[e^{-\int_t^{t+\tau} \eta_u du}] + E_t^P\left[\int_t^{t+\tau} \eta_s e^{-\int_t^s \eta_u du} r_{t+\tau} ds\right] = \int_t^{t+\tau} E_t^P\left[\eta_s e^{-\int_t^s \eta_u du} E_s^P[r_{t+\tau}]\right] ds.$$

Thus, we need the formula for $E_s^P[r_{t+\tau}]$ from the normal state to be able to calculate the involved conditional expectation. This is an affine function in the state variables:

$$E_s^P[r_{t+\tau}] = \overline{B}_L^{PE}(s, t + \tau)L_s + \overline{B}_S^{PE}(s, t + \tau)S_s + \overline{B}_C^{PE}(s, t + \tau)C_s + \overline{C}^{PE}(s, t + \tau),$$

where

$$\begin{aligned} \overline{B}_L^{PE}(s, t + \tau) &= [\exp(-K^P(t + \tau - s))]_{1,1} + [\exp(-K^P(t + \tau - s))]_{2,1}, \\ \overline{B}_S^{PE}(s, t + \tau) &= [\exp(-K^P(t + \tau - s))]_{1,2} + [\exp(-K^P(t + \tau - s))]_{2,2}, \\ \overline{B}_C^{PE}(s, t + \tau) &= [\exp(-K^P(t + \tau - s))]_{1,3} + [\exp(-K^P(t + \tau - s))]_{2,3}, \\ \overline{C}^{PE}(s, t + \tau) &= [(I - \exp(-K^P(t + \tau - s)))\theta^P]_1 + [(I - \exp(-K^P(t + \tau - s)))\theta^P]_2. \end{aligned}$$

Now, we are interested in the following expectation

$$\begin{aligned} &E_t^P\left[\eta_s e^{-\int_t^s \eta_u du} E_s^P[r_{t+\tau}]\right] \\ &= E_t^P\left[\eta_s e^{-\int_t^s \eta_u du} \left(\overline{B}_L^{PE}(s, t + \tau)L_s + \overline{B}_S^{PE}(s, t + \tau)S_s + \overline{B}_C^{PE}(s, t + \tau)C_s + \overline{C}^{PE}(s, t + \tau)\right)\right]. \end{aligned}$$

Towards this goal, Christensen (2007) has the following result.

Proposition 2:

Let the state variables X_t be described by an affine diffusion process

$$dX_t = [\mu^0 + \mu^1 X_t]dt + \Sigma D(X_t)dW_t \tag{10}$$

defined on a set $M \subset \mathbf{R}^n$. Here, $D : M \rightarrow \mathbf{R}^{n \times n}$ is assumed to have the following diagonal structure

$$D(X_t) = \begin{pmatrix} \sqrt{\gamma^1 + \delta_1^1 X_t^1 + \dots + \delta_n^1 X_t^n} & \dots & 0 \\ \vdots & \ddots & \vdots \\ 0 & \dots & \sqrt{\gamma^n + \delta_1^n X_t^1 + \dots + \delta_n^n X_t^n} \end{pmatrix}.$$

To simplify notation below, γ and δ are defined as

$$\gamma = \begin{pmatrix} \gamma^1 \\ \vdots \\ \gamma^n \end{pmatrix} \quad \text{and} \quad \delta = \begin{pmatrix} \delta_1^1 & \dots & \delta_n^1 \\ \vdots & \ddots & \vdots \\ \delta_1^n & \dots & \delta_n^n \end{pmatrix}.$$

In addition, assume the discount process to be affine in the state variables

$$R(X_t) = \rho_0 + \rho_1' X_t.$$

Then the expectation

$$G(X_t, t, T) = E \left[e^{-\int_t^T R(X_s) ds} e^{\overline{B}' X_T + \overline{C}} [X_T' \overline{D} X_T + \overline{E}' X_T + \overline{F}] \middle| \mathcal{F}_t \right],$$

where $\overline{D} \in \mathbf{R}^{n \times n}$, $\overline{B}, \overline{E} \in \mathbf{R}^n$, and $\overline{C} \in \mathbf{R}$, is given by

$$G(X_t, t, T) = \exp(B(t, T)' X_t + C(t, T)) [X_t' D(t, T) X_t + E(t, T)' X_t + F(t, T)],$$

if the following conditions are satisfied.

- (i). There exists a unique solution X_t for the stochastic differential equation (10) for all $0 \leq t \leq T$.
- (ii). There exist functions $B(t, T)$, $C(t, T)$, $D(t, T)$, $E(t, T)$, and $F(t, T)$ which are the unique solutions for the following system of first-order ordinary differential equations (ODE)⁴⁶

$$\begin{aligned} \frac{dB(t, T)}{dt} &= \rho_1 - (\mu^1)' B(t, T) - \frac{1}{2} \sum_{j=1}^n (\Sigma' B(t, T) B(t, T)' \Sigma)_{j,j} (\delta^j)', \quad B(T, T) = \overline{B}, \\ \frac{dC(t, T)}{dt} &= \rho_0 - B(t, T)' \mu^0 - \frac{1}{2} \sum_{j=1}^n (\Sigma' B(t, T) B(t, T)' \Sigma)_{j,j} \gamma^j, \quad C(T, T) = \overline{C}, \\ \frac{dD(t, T)}{dt} &= -(\mu^1)' D(t, T) - D(t, T) \mu^1 - \sum_{j=1}^n (\Sigma' B(t, T))_j (D(t, T) \Sigma)_{\cdot,j} \delta^j \\ &\quad - \sum_{j=1}^n (\Sigma' B(t, T))_j (D(t, T)' \Sigma)_{\cdot,j} \delta^j, \quad D(T, T) = \overline{D}, \\ \frac{dE(t, T)}{dt} &= -(\mu^1)' E(t, T) - D(t, T)' \mu^0 - D(t, T) \mu^0 - \sum_{j=1}^n (\Sigma' B(t, T) E(t, T)' \Sigma)_{j,j} (\delta^j)' \\ &\quad - \sum_{j=1}^n (\Sigma' D(t, T) \Sigma)_{j,j} (\delta^j)' - \sum_{j=1}^n (\Sigma' B(t, T))_j (D(t, T) \Sigma)_{\cdot,j} \gamma^j \\ &\quad - \sum_{j=1}^n (\Sigma' B(t, T))_j (D(t, T)' \Sigma)_{\cdot,j} \gamma^j, \quad E(T, T) = \overline{E}, \\ \frac{dF(t, T)}{dt} &= -E(t, T)' \mu^0 - \sum_{j=1}^n (\Sigma' D(t, T) \Sigma)_{j,j} \gamma^j - \sum_{j=1}^n (\Sigma' B(t, T) E(t, T)' \Sigma)_{j,j} \gamma^j, \quad F(T, T) = \overline{F}, \end{aligned}$$

⁴⁶Here, δ^j denotes the j th row of the δ -matrix.

(iii). The following technical conditions are met

(a) $E[|\Phi_T|] < \infty$,

(b) $E\left[\left(\int_0^T \eta_t \eta_t' dt\right)^{1/2}\right] < \infty$ for $\eta_t = (\Phi_t B(t, T)' + \Psi_t [E(t, T)' + X_t'(D(t, T) + D(t, T)')]) \Sigma D$,

where $\Phi_t = e^{-\int_0^t r(X_s, s) ds} e^{B(t, T)' X_t + C(t, T)} [X_t' D(t, T) X_t + E(t, T)' X_t + F(t, T)]$ and $\Psi_t = e^{-\int_0^t r(X_s, s) ds} e^{B(t, T)' X_t + C(t, T)}$ for all $0 \leq t \leq T$.

This proposition implies that it only requires the solution of a system of ODEs to calculate conditional short rate expectations in the zero-bound state. In this paper, this is done by standard fourth-order Runge Kutta methods.

In the zero-bound state, the joint P -dynamics of the state variables are given by

$$\begin{aligned} \begin{pmatrix} dL_t \\ dS_t \\ dC_t \\ d\eta_t \end{pmatrix} &= \begin{pmatrix} \kappa_{11}^P & \kappa_{12}^P & \kappa_{13}^P & \kappa_{14}^P \\ \kappa_{21}^P & \kappa_{22}^P & \kappa_{23}^P & \kappa_{24}^P \\ \kappa_{31}^P & \kappa_{32}^P & \kappa_{33}^P & \kappa_{34}^P \\ 0 & 0 & 0 & \kappa_{44}^P \end{pmatrix} \begin{bmatrix} \begin{pmatrix} \theta_1^P \\ \theta_2^P \\ \theta_3^P \\ \theta_4^P \end{pmatrix} \\ - \begin{pmatrix} L_t \\ S_t \\ C_t \\ \eta_t \end{pmatrix} \end{bmatrix} dt \\ &+ \begin{pmatrix} \sigma_L & 0 & 0 & 0 \\ 0 & \sigma_S & 0 & 0 \\ 0 & 0 & \sigma_C & 0 \\ 0 & 0 & 0 & \sigma_\eta \end{pmatrix} \begin{pmatrix} \sqrt{1} & 0 & 0 & 0 \\ 0 & \sqrt{1} & 0 & 0 \\ 0 & 0 & \sqrt{1} & 0 \\ 0 & 0 & 0 & \sqrt{\eta_t} \end{pmatrix} \begin{pmatrix} dW_t^{L,P} \\ dW_t^{S,P} \\ dW_t^{C,P} \\ dW_t^{\eta,P} \end{pmatrix}. \end{aligned}$$

Thus, the vectors and matrices describing the P -dynamics of the state variables and appearing in the system of ODEs are given by:

$$\begin{aligned} \rho_0 = 0, \quad \rho_1 &= \begin{pmatrix} 0 \\ 0 \\ 0 \\ 1 \end{pmatrix}, \quad \mu^0 = \begin{pmatrix} \kappa_{11}^P & \kappa_{12}^P & \kappa_{13}^P & \kappa_{14}^P \\ \kappa_{21}^P & \kappa_{22}^P & \kappa_{23}^P & \kappa_{24}^P \\ \kappa_{31}^P & \kappa_{32}^P & \kappa_{33}^P & \kappa_{34}^P \\ 0 & 0 & 0 & \kappa_{44}^P \end{pmatrix} \begin{pmatrix} \theta_1^P \\ \theta_2^P \\ \theta_3^P \\ \theta_4^P \end{pmatrix}, \quad \mu^1 = - \begin{pmatrix} \kappa_{11}^P & \kappa_{12}^P & \kappa_{13}^P & \kappa_{14}^P \\ \kappa_{21}^P & \kappa_{22}^P & \kappa_{23}^P & \kappa_{24}^P \\ \kappa_{31}^P & \kappa_{32}^P & \kappa_{33}^P & \kappa_{34}^P \\ 0 & 0 & 0 & \kappa_{44}^P \end{pmatrix}, \\ \Sigma &= \begin{pmatrix} \sigma_L & 0 & 0 & 0 \\ 0 & \sigma_S & 0 & 0 \\ 0 & 0 & \sigma_C & 0 \\ 0 & 0 & 0 & \sigma_\eta \end{pmatrix}, \quad \gamma = \begin{pmatrix} 1 \\ 1 \\ 1 \\ 0 \end{pmatrix}, \quad \text{and} \quad \delta = \begin{pmatrix} 0 & 0 & 0 & 0 \\ 0 & 0 & 0 & 0 \\ 0 & 0 & 0 & 0 \\ 0 & 0 & 0 & 1 \end{pmatrix}. \end{aligned}$$

Finally, the boundary conditions in the system of ODEs in Proposition 2 are given by:

$$\begin{aligned} \bar{B} &= \begin{pmatrix} 0 \\ 0 \\ 0 \\ 0 \end{pmatrix}, \quad \bar{C} = 0, \quad \bar{D} = \begin{pmatrix} 0 & 0 & 0 & \frac{1}{2} \bar{B}_L^{PE}(s, t + \tau) \\ 0 & 0 & 0 & \frac{1}{2} \bar{B}_S^{PE}(s, t + \tau) \\ 0 & 0 & 0 & \frac{1}{2} \bar{B}_C^{PE}(s, t + \tau) \\ \frac{1}{2} \bar{B}_L^{PE}(s, t + \tau) & \frac{1}{2} \bar{B}_S^{PE}(s, t + \tau) & \frac{1}{2} \bar{B}_C^{PE}(s, t + \tau) & 0 \end{pmatrix}, \\ \bar{E} &= \begin{pmatrix} 0 \\ 0 \\ 0 \\ \bar{C}^{PE}(s, t + \tau) \end{pmatrix}, \quad \bar{F} = 0. \end{aligned}$$

Now, denote the solution to the system of ODEs in Proposition 2 by $B^{PE}(t, s, t + \tau)$, $C^{PE}(t, s, t + \tau)$,

$D^{PE}(t, s, t + \tau)$, $E^{PE}(t, s, t + \tau)$, and $F^{PE}(t, s, t + \tau)$, and it follows that

$$\begin{aligned} & E_t^P \left[\eta_s e^{-\int_t^s \eta_u du} E_s^P [r_{t+\tau}] \right] \\ = & E_t^P \left[\eta_s e^{-\int_t^s \eta_u du} \left(\overline{B}_L^{PE}(s, t + \tau) L_s + \overline{B}_S^{PE}(s, t + \tau) S_s + \overline{B}_C^{PE}(s, t + \tau) C_s + \overline{C}^{PE}(s, t + \tau) \right) \right] \\ = & \exp \left(B^{PE}(t, s, t + \tau)' X_t + C^{PE}(t, s, t + \tau) \right) \left[X_t' D^{PE}(t, s, t + \tau) X_t + E^{PE}(t, s, t + \tau)' X_t + F^{PE}(t, s, t + \tau) \right]. \end{aligned}$$

Thus, the expected instantaneous short rate in the zero-bound state is given by

$$\begin{aligned} E_t^P [r_{t+\tau}] &= \int_t^{t+\tau} E_t^P \left[\eta_s e^{-\int_t^s \eta_u du} E_s^P [r_{t+\tau}] \right] ds \\ &= \int_t^{t+\tau} \exp \left(B^{PE}(t, s, t + \tau)' X_t + C^{PE}(t, s, t + \tau) \right) \\ &\quad \times \left[X_t' D^{PE}(t, s, t + \tau) X_t + E^{PE}(t, s, t + \tau)' X_t + F^{PE}(t, s, t + \tau) \right] ds. \end{aligned}$$

Appendix C: Term Premiums in the Regime-Switching Model

In general, the term premium part of the yield on a zero-coupon bond with maturity in τ years is defined as

$$TP_t(\tau) = y(t, t + \tau) - \frac{1}{\tau} \int_t^{t+\tau} E_t^P [r_s] ds.$$

In the normal state, the term premium takes its usual form

$$TP_t^N(\tau) = y^N(t, t + \tau) - \frac{1}{\tau} \int_t^{t+\tau} E_t^P [r_s] ds, \quad (11)$$

where the instantaneous short rate is the sum of the first two factors

$$r_t = L_t + S_t.$$

In the zero-bound state, the formula for the term premium is given by

$$\begin{aligned} TP_t^Z(\tau) &= y^Z(t, t + \tau) - \frac{1}{\tau} \left(0 \cdot E_t^P [e^{-\int_t^{t+\tau} \eta_u du}] + E_t^P \left[\int_t^{t+\tau} \eta_s e^{-\int_t^s \eta_u du} \int_s^{t+\tau} r_u du ds \right] \right) \\ &= y^Z(t, t + \tau) - \frac{1}{\tau} \int_t^{t+\tau} E_t^P \left[\eta_s e^{-\int_t^s \eta_u du} E_s^P \left[\int_s^{t+\tau} r_u du \right] \right] ds. \end{aligned}$$

Thus, we need the formula for $E_s^P [\int_s^{t+\tau} r_u du]$ from the normal state to be able to calculate the involved conditional expectation efficiently.

Define

$$Y_{0,t} = \int_0^t r_u du = \int_0^t (L_u + S_u) du \quad \Rightarrow \quad dY_{0,t} = (L_t + S_t) dt.$$

Adding the $Y_{0,t}$ -process to the dynamics of the state variables in the normal state, leaves us with an augmented

system of stochastic differential equations given by

$$\begin{pmatrix} dL_t \\ dS_t \\ dC_t \\ dY_{0,t} \end{pmatrix} = \begin{pmatrix} \kappa_{11}^P & \kappa_{12}^P & \kappa_{13}^P & 0 \\ \kappa_{21}^P & \kappa_{22}^P & \kappa_{23}^P & 0 \\ \kappa_{31}^P & \kappa_{32}^P & \kappa_{33}^P & 0 \\ 0 & 0 & 0 & 0 \end{pmatrix} \begin{pmatrix} \theta_1^P \\ \theta_2^P \\ \theta_3^P \\ 0 \end{pmatrix} - \begin{pmatrix} \kappa_{11}^P & \kappa_{12}^P & \kappa_{13}^P & 0 \\ \kappa_{21}^P & \kappa_{22}^P & \kappa_{23}^P & 0 \\ \kappa_{31}^P & \kappa_{32}^P & \kappa_{33}^P & 0 \\ -1 & -1 & 0 & 0 \end{pmatrix} \begin{pmatrix} L_t \\ S_t \\ C_t \\ Y_{0,t} \end{pmatrix} dt \\ + \begin{pmatrix} \sigma_L & 0 & 0 & 0 \\ 0 & \sigma_S & 0 & 0 \\ 0 & 0 & \sigma_C & 0 \\ 0 & 0 & 0 & 0 \end{pmatrix} \begin{pmatrix} dW_t^{L,P} \\ dW_t^{S,P} \\ dW_t^{C,P} \\ dW_t^{Y,P} \end{pmatrix},$$

where $Z_{0,t} = (L_t, S_t, C_t, Y_{0,t})$ represents the augmented state vector.

First, we define vectors and matrices related to the model dynamics as follows

$$\rho_0 = 0, \quad \rho_1 = \begin{pmatrix} 0 \\ 0 \\ 0 \\ 0 \end{pmatrix}, \quad \mu^0 = \begin{pmatrix} \kappa_{11}^P & \kappa_{12}^P & \kappa_{13}^P & 0 \\ \kappa_{21}^P & \kappa_{22}^P & \kappa_{23}^P & 0 \\ \kappa_{31}^P & \kappa_{32}^P & \kappa_{33}^P & 0 \\ 0 & 0 & 0 & 0 \end{pmatrix} \begin{pmatrix} \theta_1^P \\ \theta_2^P \\ \theta_3^P \\ 0 \end{pmatrix}, \quad \mu^1 = - \begin{pmatrix} \kappa_{11}^P & \kappa_{12}^P & \kappa_{13}^P & 0 \\ \kappa_{21}^P & \kappa_{22}^P & \kappa_{23}^P & 0 \\ \kappa_{31}^P & \kappa_{32}^P & \kappa_{33}^P & 0 \\ -1 & -1 & 0 & 0 \end{pmatrix}, \\ \Sigma = \begin{pmatrix} \sigma_L & 0 & 0 & 0 \\ 0 & \sigma_S & 0 & 0 \\ 0 & 0 & \sigma_C & 0 \\ 0 & 0 & 0 & 0 \end{pmatrix}, \quad \gamma = \begin{pmatrix} 1 \\ 1 \\ 1 \\ 1 \end{pmatrix}, \quad \text{and} \quad \delta = \begin{pmatrix} 0 & 0 & 0 & 0 \\ 0 & 0 & 0 & 0 \\ 0 & 0 & 0 & 0 \\ 0 & 0 & 0 & 0 \end{pmatrix}.$$

Second, we define the boundary conditions as follows

$$\bar{B} = \begin{pmatrix} 0 \\ 0 \\ 0 \\ 0 \end{pmatrix}, \quad \bar{C} = 0, \quad \bar{D} = 0, \quad \bar{E} = \begin{pmatrix} 0 \\ 0 \\ 0 \\ 1 \end{pmatrix}, \quad \bar{F} = 0.$$

Now, Proposition 2 implies that

$$\begin{aligned} E_0^P \left[\int_0^t r_u du \right] &= E_0^P [Y_{0,t}] \\ &= E_0^P \left[e^{-\int_0^t (\rho_0 + \rho_1 Z_{0,s}) ds} e^{\bar{B}' Z_{0,t} + \bar{C}} [Z'_{0,t} \bar{D} Z_{0,t} + \bar{E}' Z_{0,t} + \bar{F}] \right] \\ &= \exp(B(0,t)' Z_{0,0} + C(0,t)) [Z'_{0,0} \bar{D}(0,t) Z_{0,0} + E(0,t)' Z_{0,0} + F(0,t)], \end{aligned}$$

where $B(0,t)$, $C(0,t)$, $D(0,t)$, $E(0,t)$, and $F(0,t)$ are the unique solutions to the system of ODEs provided in the proposition.

To summarize this intermediate step, the requisite conditional expectation is an affine function in the state variables:⁴⁷

$$E_s^P \left[\int_s^{t+\tau} r_u du \right] = \bar{B}_L^{TP}(s, t+\tau) L_s + \bar{B}_S^{TP}(s, t+\tau) S_s + \bar{B}_C^{TP}(s, t+\tau) C_s + \bar{C}^{TP}(s, t+\tau),$$

⁴⁷Here, we have used that $B(0,t) = 0$, $C(0,t) = 0$, and $D(0,t) = 0$ for all $t > 0$. In addition, we have used that $Y_{t,t} = 0$ for any t .

where

$$\begin{aligned}\overline{B}_L^{TP}(s, t + \tau) &= E(0, t + \tau - s)_1, \\ \overline{B}_S^{TP}(s, t + \tau) &= E(0, t + \tau - s)_2, \\ \overline{B}_C^{TP}(s, t + \tau) &= E(0, t + \tau - s)_3, \\ \overline{C}^{TP}(s, t + \tau) &= F(0, t + \tau - s).\end{aligned}$$

Now, we are interested in the following expectation

$$\begin{aligned}& E_t^P \left[\eta_s e^{-\int_t^s \eta_u du} E_s^P \left[\int_s^{t+\tau} r_u du \right] \right] \\ &= E_t^P \left[\eta_s e^{-\int_t^s \eta_u du} \left(\overline{B}_L^{TP}(s, t + \tau) L_s + \overline{B}_S^{TP}(s, t + \tau) S_s + \overline{B}_C^{TP}(s, t + \tau) C_s + \overline{C}^{TP}(s, t + \tau) \right) \right],\end{aligned}$$

where Proposition 2 can again be applied.

If we continue to assume the unrestricted specification of the joint P -dynamics of the state variables in the zero-bound state, the vectors and matrices describing the P -dynamics of the state variables and appearing in the system of ODEs in Proposition 2 are given by:

$$\begin{aligned}\rho_0 = 0, \quad \rho_1 &= \begin{pmatrix} 0 \\ 0 \\ 0 \\ 1 \end{pmatrix}, \quad \mu^0 = \begin{pmatrix} \kappa_{11}^P & \kappa_{12}^P & \kappa_{13}^P & \kappa_{14}^P \\ \kappa_{21}^P & \kappa_{22}^P & \kappa_{23}^P & \kappa_{24}^P \\ \kappa_{31}^P & \kappa_{32}^P & \kappa_{33}^P & \kappa_{34}^P \\ 0 & 0 & 0 & \kappa_{44}^P \end{pmatrix} \begin{pmatrix} \theta_1^P \\ \theta_2^P \\ \theta_3^P \\ \theta_4^P \end{pmatrix}, \quad \mu^1 = - \begin{pmatrix} \kappa_{11}^P & \kappa_{12}^P & \kappa_{13}^P & \kappa_{14}^P \\ \kappa_{21}^P & \kappa_{22}^P & \kappa_{23}^P & \kappa_{24}^P \\ \kappa_{31}^P & \kappa_{32}^P & \kappa_{33}^P & \kappa_{34}^P \\ 0 & 0 & 0 & \kappa_{44}^P \end{pmatrix}, \\ \Sigma &= \begin{pmatrix} \sigma_L & 0 & 0 & 0 \\ 0 & \sigma_S & 0 & 0 \\ 0 & 0 & \sigma_C & 0 \\ 0 & 0 & 0 & \sigma_\eta \end{pmatrix}, \quad \gamma = \begin{pmatrix} 1 \\ 1 \\ 1 \\ 0 \end{pmatrix}, \quad \text{and} \quad \delta = \begin{pmatrix} 0 & 0 & 0 & 0 \\ 0 & 0 & 0 & 0 \\ 0 & 0 & 0 & 0 \\ 0 & 0 & 0 & 1 \end{pmatrix}.\end{aligned}$$

Finally, the boundary conditions are given by:

$$\begin{aligned}\overline{B} &= \begin{pmatrix} 0 \\ 0 \\ 0 \\ 0 \end{pmatrix}, \quad \overline{C} = 0, \quad \overline{D} = \begin{pmatrix} 0 & 0 & 0 & \frac{1}{2} \overline{B}_L^{TP}(s, t + \tau) \\ 0 & 0 & 0 & \frac{1}{2} \overline{B}_S^{TP}(s, t + \tau) \\ 0 & 0 & 0 & \frac{1}{2} \overline{B}_C^{TP}(s, t + \tau) \\ \frac{1}{2} \overline{B}_L^{TP}(s, t + \tau) & \frac{1}{2} \overline{B}_S^{TP}(s, t + \tau) & \frac{1}{2} \overline{B}_C^{TP}(s, t + \tau) & 0 \end{pmatrix}, \\ \overline{E} &= \begin{pmatrix} 0 \\ 0 \\ 0 \\ \overline{C}^{TP}(s, t + \tau) \end{pmatrix}, \quad \overline{F} = 0.\end{aligned}$$

Now, denote the solution to the system of ODEs in Proposition 2 by $B^{TP}(t, s, t + \tau)$, $C^{TP}(t, s, t + \tau)$, $D^{TP}(t, s, t + \tau)$, $E^{TP}(t, s, t + \tau)$, and $F^{TP}(t, s, t + \tau)$, and it follows that

$$\begin{aligned}& E_t^P \left[\eta_s e^{-\int_t^s \eta_u du} E_s^P \left[\int_s^{t+\tau} r_u du \right] \right] \\ &= E_t^P \left[\eta_s e^{-\int_t^s \eta_u du} \left(\overline{B}_L^{TP}(s, t + \tau) L_s + \overline{B}_S^{TP}(s, t + \tau) S_s + \overline{B}_C^{TP}(s, t + \tau) C_s + \overline{C}^{TP}(s, t + \tau) \right) \right] \\ &= \exp \left(B^{TP}(t, s, t + \tau)' X_t + C^{TP}(t, s, t + \tau) \right) \left[X_t' D^{TP}(t, s, t + \tau) X_t + E^{TP}(t, s, t + \tau)' X_t + F^{TP}(t, s, t + \tau) \right].\end{aligned}$$

Thus, the term premium in the zero-bound state is calculated as

$$\begin{aligned}
TP_t^Z(\tau) &= y^Z(t, t+\tau) - \frac{1}{\tau} \int_t^{t+\tau} E_t^P \left[\eta_s e^{-\int_t^s \eta_u du} E_s^P \left[\int_s^{t+\tau} r_u du \right] \right] ds \\
&= y^Z(t, t+\tau) - \frac{1}{\tau} \int_t^{t+\tau} \exp \left(B^{TP}(t, s, t+\tau)' X_t + C^{TP}(t, s, t+\tau) \right) \\
&\quad \times \left[X_t' D^{TP}(t, s, t+\tau) X_t + E^{TP}(t, s, t+\tau)' X_t + F^{TP}(t, s, t+\tau) \right] ds.
\end{aligned}$$

References

- Andersen, Torben G. and Luca Benzoni, 2010, “Do Bonds Span Volatility Risk in the U.S. Treasury Market? A Specification Test for Affine Term Structure Models,” *Journal of Finance*, Vol. 65, No. 2, 603-653.
- Bauer, Michael D. and Glenn D. Rudebusch, 2013, “The Signaling Channel for Federal Reserve Bond Purchases,” *International Journal of Central Banking*, forthcoming.
- Bauer, Michael D. and Glenn D. Rudebusch, 2014, “Monetary Policy Expectations at the Zero Lower Bound,” Working Paper 2013-18, Federal Reserve Bank of San Francisco.
- Bauer, Michael D., Glenn D. Rudebusch, and Jing (Cynthia) Wu, 2012, “Correcting Estimation Bias in Dynamic Term Structure Models,” *Journal of Business and Economic Statistics*, Vol. 30, No. 3, 454-467.
- Black, Fisher, 1995, “Interest Rates as Options,” *Journal of Finance*, Vol. 50, No. 7, 1371-1376.
- Cahill, Michael E., Stefania D’Amico, Canlin Li, and John S. Sears, 2013, “Duration Risk versus Local Supply Channel in Treasury Yields: Evidence from the Federal Reserve’s Asset Purchase Announcements,” Finance and Economics Discussion Series Working Paper 2013-35, Board of Governors of the Federal Reserve System.
- Cheridito, Patrick, Damir Filipović, and Robert L. Kimmel, 2007, “Market Price of Risk Specifications for Affine Models: Theory and Evidence,” *Journal of Financial Economics*, Vol. 83, No. 1, 123-170.
- Christensen, Jens H. E., 2007, “Default and Recovery Risk Modeling and Estimation,” PhD Dissertation, PhD Series 18.2007, Department of Finance, Copenhagen Business School.
- Christensen, Jens H. E., 2014, “When Will the Fed End Its Zero Rate Policy?,” Federal Reserve Bank of San Francisco, *Economic Letter* 2014-04.
- Christensen, Jens H. E., Francis X. Diebold, and Glenn D. Rudebusch, 2011, “The Affine Arbitrage-Free Class of Nelson-Siegel Term Structure Models,” *Journal of Econometrics*, Vol. 164, No. 1, 4-20.
- Christensen, Jens H. E., Jose A. Lopez, and Glenn D. Rudebusch, 2010, “Inflation Expectations and Risk Premiums in an Arbitrage-Free Model of Nominal and Real Bond Yields,” *Journal of Money, Credit and Banking*, Supplement to Vol. 42, No. 6, 143-178.

- Christensen, Jens H. E., Jose A. Lopez, and Glenn D. Rudebusch, 2012, "Pricing Deflation Risk with U.S. Treasury Yields," Working Paper 2012-07, Federal Reserve Bank of San Francisco.
- Christensen, Jens H. E., Jose A. Lopez, and Glenn D. Rudebusch, 2014, "Can Spanned Term Structure Factors Drive Stochastic Yield Volatility?," Working Paper 2014-03, Federal Reserve Bank of San Francisco.
- Christensen, Jens H. E. and Glenn D. Rudebusch, 2012, "The Response of Interest Rates to U.S. and U.K. Quantitative Easing," *Economic Journal*, Vol. 122, F385-F414.
- Christensen, Jens H. E. and Glenn D. Rudebusch, 2013, "Modeling Yields at the Zero Lower Bound: Are Shadow Rates the Solution?," Working Paper 2013-39, Federal Reserve Bank of San Francisco.
- Christensen, Jens H. E. and Glenn D. Rudebusch, 2014, "Estimating Shadow-Rate Term Structure Models with Near-Zero Yields," *Journal of Financial Econometrics*, forthcoming.
- Cochrane, John and Monika Piazzesi, 2005, "Bond Risk Premia," *American Economic Review*, Vol. 94, No. 1, 138-160.
- Collin-Dufresne, Pierre, Robert S. Goldstein, and Chris S. Jones, 2009, "Can Interest Rate Volatility Be Extracted from the Cross-Section of Bond Yields?," *Journal of Financial Economics*, Vol. 94, No. 1, 47-66.
- Dai, Qiang, Kenneth J. Singleton, and Wei Yang, 2007, "Regime Shifts in a Dynamic Term Structure Model of U.S. Treasury Bond Yields," *Review of Financial Studies*, Vol. 20, No. 5, 1669-1706.
- Diebold, Francis X. and Glenn D. Rudebusch, 2013, *Yield Curve Modeling and Forecasting: The Dynamic Nelson-Siegel Approach*, Princeton, NJ: Princeton University Press.
- Driessen, Joost, 2005, "Is Default Event Risk Priced in Corporate Bonds?" *Review of Financial Studies*, Vol. 18, No. 1, 165-195.
- Duffee, Gregory R., 1999, "Estimating the Price of Default Risk," *Review of Financial Studies*, Vol. 12, No. 1, 197-226.
- Duffee, Gregory R., 2011, "Information in (and not in) the Term Structure," *Review of Financial Studies*, Vol. 24, No. 9, 2895-2934.
- Duffie, Darrell and David Lando, 2001, "Term Structures of Credit Spreads with Incomplete Accounting Information," *Econometrica*, Vol. 69, No. 3, 633-664.

- Duffie, Darrell and Kenneth J. Singleton, 1999, "Modeling Term Structures of Defaultable Bonds," *Review of Financial Studies*, Vol. 12, No. 4, 687-720.
- Feldhütter, Peter and David Lando, 2008, "Decomposing Swap Spreads," *Journal of Financial Economics*, Vol. 88, No. 2, 375-405.
- Fisher, Mark and Christian Gilles, 1996, "Term Premia in Exponential-Affine Models of the Term Structure," unpublished manuscript, Board of Governors of the Federal Reserve System.
- Gürkaynak, Refet S., Brian Sack, and Jonathan H. Wright, 2007, "The U.S. Treasury Yield Curve: 1961 to the Present," *Journal of Monetary Economics*, Vol. 54, No. 8, 2291-2304.
- Harvey, A.C., 1989, *Forecasting, Structural Time Series Models and the Kalman Filter*, Cambridge: Cambridge University Press.
- Jacobs, Kris and Lofti Karoui, 2009, "Conditional Volatility in Affine Term Structure Models: Evidence from Treasury and Swap Markets," *Journal of Financial Economics*, Vol. 91, No. 3, 288-318.
- Joslin, Scott, Kenneth J. Singleton, and Haoxiang Zhu, 2011, "A New Perspective on Gaussian Dynamic Term Structure Models," *Review of Financial Studies*, Vol. 24, No. 3, 926-970.
- Kim, Don H. and Athanasios Orphanides, 2012, "Term Structure Estimation with Survey Data on Interest Rate Forecasts," *Journal of Financial and Quantitative Analysis*, Vol. 47, No. 1, 241-272.
- Kim, Don H. and Kenneth J. Singleton, 2012, "Term Structure Models and the Zero Bound: An Empirical Investigation of Japanese Yields," *Journal of Econometrics*, Vol. 170, No. 1, 32-49.
- Kim, Don H. and Jonathan H. Wright, 2005, "An Arbitrage-Free Three-Factor Term Structure Model and the Recent Behavior of Long-Term Yields and Distant-Horizon Forward Rates," Working Paper Finance and Economics Discussion Series 2005-33, Board of Governors of the Federal Reserve System.
- Koeda, Junko, 2013, "Endogenous Monetary Policy Shifts and the Term Structure: Evidence from Japanese Government Bond Yields," Manuscript, Faculty of Economics, University of Tokyo.

- Krippner, Leo, 2013a, "A Theoretical Foundation for the Nelson and Siegel Class of Yield Curve Models," *Journal of Applied Econometrics*, forthcoming.
- Krippner, Leo, 2013b, "A Tractable Framework for Zero Lower Bound Gaussian Term Structure Models," Discussion Paper 2013-02, Reserve Bank of New Zealand.
- Li, Canlin and Min Wei, 2013, "Term Structure Modeling with Supply Factors and the Federal Reserve's Large-Scale Asset Purchase Programs," *International Journal of Central Banking*, Vol. 9, No. 1, 3-39.
- Litterman, R. and J. A. Scheinkman, 1991, "Common Factors Affecting Bond Returns," *Journal of Fixed Income*, Vol. 1, No. 1, 62-74.
- Monfort, Alain, Fulvio Pegoraro, Jean-Paul Renne, and Guillaume Roussellet, 2014 "Staying at Zero with Affine Processes: A New Dynamic Term Structure Model," Manuscript. Banque de France.
- Nelson, Charles R. and Andrew F. Siegel, 1987, "Parsimonious Modeling of Yield Curves," *Journal of Business*, Vol. 60, No. 4, 473-489.
- Piazzesi, Monika, 2005, "Bond Yields and the Federal Reserve," *Journal of Political Economy*, Vol. 113, No. 2, 311-344.
- Piazzesi, Monika and Eric T. Swanson, 2008, "Futures Prices as Risk-Adjusted Forecasts of Monetary Policy," *Journal of Monetary Economics*, Vol. 55, No. 4, 677-691.
- Swanson, Eric T. and John C. Williams, 2014, "Measuring the Effect of the Zero Lower Bound on Medium- and Longer-Term Interest Rates," *American Economic Review*, forthcoming.
- Wu, Jing (Cynthia) and Fan Dora Xia, 2014, "Measuring the Macroeconomic Impact of Monetary Policy at the Zero Lower Bound," Manuscript. Chicago Booth School of Business.